

1 **VIP plasma levels associate with survival in severe COVID-19 patients,**
2 **correlating with protective effects in SARS-CoV-2-infected cells.**

3 Jairo R. Temerozo^{1,10,*}, Carolina Q. Sacramento^{2,3}, Natalia Fintelman-Rodrigues^{2,3},
4 Camila R. R. Pão², Caroline S. de Freitas^{2,3}, Suelen Silva Gomes Dias², André C.
5 Ferreira^{2,3,4}, Mayara Mattos^{2,3}, Vinicius Cardoso Soares^{2,5}, Lívia Teixeira²,
6 Isaclaudia G. Azevedo-Quintanilha², Eugenio D. Hottz⁶, Pedro Kurtz^{7,8}, Fernando
7 A. Bozza^{8,9}, Patrícia T. Bozza², Thiago Moreno L. Souza^{2,3}, Dumith Chequer Bou-
8 Habib^{1,10,*}

9 ¹Laboratory on Thymus Research, Oswaldo Cruz Institute, Fiocruz, Rio de Janeiro, RJ,
10 Brazil; ²Laboratory of Immunopharmacology, Oswaldo Cruz Institute, Fiocruz, Rio de
11 Janeiro, RJ, Brazil; ³National Institute for Science and Technology on Innovation in
12 Diseases of Neglected Populations (INCT/IDPN), Center for Technological Development in
13 Health (CDTS), Fiocruz, Rio de Janeiro, RJ, Brazil; ⁴Iguaçu University, Nova Iguaçu, RJ,
14 Brazil; ⁵Program of Immunology and Inflammation, Federal University of Rio de Janeiro,
15 UFRJ, Rio de Janeiro, RJ, Brazil; ⁶Laboratory of Immunothrombosis, Department of
16 Biochemistry, Federal University of Juiz de Fora (UFJF), Juiz de Fora, Minas Gerais, Brazil;
17 ⁷Paulo Niemeyer State Brain Institute, Rio de Janeiro, RJ, Brazil; ⁸D'Or Institute for
18 Research and Education, Rio de Janeiro, RJ, Brazil; ⁹Evandro Chagas National Institute of
19 Infectious Diseases, Fiocruz, Rio de Janeiro, RJ, Brazil; ¹⁰National Institute for Science and
20 Technology on Neuroimmunomodulation, Oswaldo Cruz Institute, Fiocruz, Rio de Janeiro,
21 RJ, Brazil.

22 **Short Title:** Protective effects of VIP and PACAP in SARS-CoV-2 infection

23 **Corresponding authors:** Jairo R. Temerozo and Dumith Chequer Bou-Habib
24 Laboratório de Pesquisas sobre o Timo, Instituto Oswaldo Cruz/Fiocruz
25 Av. Brasil, 4365 - Manguinhos - 21040-360 - Pav. Leônidas Deane – sala 510
26 Rio de Janeiro, RJ, Brazil – Tel: +55 21 3865-8139
27 E-mail: jairo.jrt@gmail.com, dumith@ioc.fiocruz.br, dumith.chequer@gmail.com

28 **Number of Tables:** 1

29 **Number of Figures:** 7

30 **Word count:** 5813

31 **Key words:** SARS-CoV-2; COVID-19; VIP; PACAP; Neuropeptides

32 **Abstract**

33 Infection by SARS-CoV-2 may elicit uncontrolled and damaging inflammatory
34 responses. Thus, it is critical to identify compounds able to inhibit virus replication
35 and thwart the inflammatory reaction. Here, we show that the plasma levels of the
36 immunoregulatory neuropeptide VIP are elevated in patients with severe COVID-
37 19, correlating with reduced inflammatory mediators and with survival on those
38 patients. In vitro, VIP and PACAP, highly similar neuropeptides, decreased the
39 SARS-CoV-2 genome replication in human monocytes and viral production in lung
40 epithelial cells, also reducing cell death. Both neuropeptides inhibited the production
41 of proinflammatory mediators in lung epithelial cells and in monocytes. VIP and
42 PACAP prevented in monocytes the SARS-CoV-2-induced activation of NF- κ B and
43 SREBP1 and SREBP2, transcription factors involved in proinflammatory reactions
44 and lipid metabolism, respectively. They also promoted CREB activation, a
45 transcription factor with antiapoptotic activity and negative regulator of NF- κ B.
46 Specific inhibition of NF- κ B and SREBP1/2 reproduced the anti-inflammatory,
47 antiviral and cell death protection effects of VIP and PACAP. Our results support
48 further clinical investigations of these neuropeptides against COVID-19.

49 **Introduction**

50 Individuals with coronavirus disease 2019 (COVID-19), caused by the severe
51 acute respiratory syndrome coronavirus 2 (SARS-CoV-2) [1], may present
52 asymptomatic or mild disease to severe lung inflammation and acute respiratory
53 distress syndrome (ARDS) [2,3], besides a variety of extrapulmonary manifestations
54 [4]. Severe SARS-CoV-2 infection is characterized by elevated serum levels of
55 proinflammatory mediators (hypercytokinemia, also known as cytokine storm) such

56 as, for example, IL-2, IL-6, TNF, IL-8, IL-1 β , IFN- γ [2,3,5,6]. The dysregulated
57 immune response and production of cytokines and chemokines are hallmarks of
58 SARS-CoV-2 infection and have been pointed as the main cause of the severe lung
59 damage and unfavorable clinical progression of patients with COVID-19 [3–8]. Also,
60 the in vivo formation of neutrophil extracellular traps (NETs) in the lungs, SARS-
61 CoV-2-induced inflammasome activation and cell death by pyroptosis, have also
62 been considered as risk factors in critically ill COVID-19 patients [9–14].

63 During the inflammatory response to human pathogenic coronaviruses,
64 circulating neutrophils and monocytes migrate and infiltrate the lungs [15,16] and
65 other organs, contributing to potentiate and perpetuate the inflammation and
66 eventually exacerbating the tissue damage [17–19]. Previous studies showed that
67 MERS-CoV- and SARS-CoV-infected macrophages produce high levels of pro-
68 inflammatory cytokines and chemokines [20,21], and, more recently, that lung
69 monocytes from severe pneumonia caused by SARS-CoV-2 are potent producers
70 of TNF- α and IL-6, whose levels were increased in the serum of the same patients
71 [7]. Also, we and other authors have found that SARS-CoV-2 induces
72 inflammasome activation and cell death by pyroptosis in monocytes, either by
73 experimental or natural infection, which are associated with lung inflammation and
74 are risk factors in critically ill COVID-19 patients [13,14].

75 Thus, it is critical to identify agents able to prevent the infection and
76 concurrently thwart the prototypical dysregulated inflammatory reaction and tissue
77 lesions secondary to SARS-CoV-2 infection. In this work, we evaluated whether the
78 neuropeptides Vasoactive Intestinal Peptide (VIP) and Pituitary Adenylate Cyclase-
79 Activating Polypeptide (PACAP) can present protective effects in SARS-CoV-2

80 infection. VIP and PACAP share many biological properties through their interaction
81 with the G protein-coupled receptors VPAC1, VPAC2 and PAC1 [22], which are
82 systemically distributed. They have well-characterized regulatory effects on the
83 immune system and anti-inflammatory properties, including control of cell activation
84 and differentiation, down-regulation of inflammatory cytokines and reactive oxygen
85 species and induction of the anti-inflammatory cytokine IL-10 [23–28]. Based on
86 their consistent anti-inflammatory and pro-homeostatic activities, both
87 neuropeptides have been considered as promising therapeutic agents for
88 autoimmune disorders and chronic inflammatory illnesses [29–32]. Therefore,
89 based on the well-known properties of both neuropeptides to regulate inflammatory
90 reactions, and on the dysregulated immune responses that affect COVID-19
91 patients, we investigated whether they could present protective roles during SARS-
92 CoV-2 infection. We report here that VIP levels are elevated in the plasma of
93 individuals with severe manifestations of COVID-19, which correlated with survival
94 on critically ill patients. We also verified, in in vitro assays, that VIP and PACAP
95 inhibit the production of proinflammatory mediators in SARS-CoV-2-infected
96 monocytes and lung epithelial cells; and reduced viral production and cell death.

97 **Materials and Methods**

98 **Cells, virus and reagents.** African green monkey kidney cells (Vero, subtype E6)
99 and human lung epithelial cell lines (Calu-3) were expanded in high glucose DMEM
100 (Vero) or MEM (Calu-3) with 10% fetal bovine serum (FBS; Merck), with 100 U/mL
101 penicillin and 100 µg/mL streptomycin (Pen/Strep; Gibco) at 37°C in a humidified
102 atmosphere with 5% CO₂. Peripheral blood mononuclear cells (PBMCs) were
103 isolated by density gradient centrifugation (Ficoll-Paque, GE Healthcare) from buffy-

104 coat preparations of blood from healthy donors. PBMCs (2×10^6 cells) were plated
105 onto 48-well plates (NalgeNunc) in RPMI-1640 with 5% inactivated male human AB
106 serum (Merck) for 3 hours. Non-adherent cells were removed and monocytes were
107 maintained in DMEM (low-glucose) with 5% human serum and 100 U/mL penicillin
108 and 100 μ g/mL streptomycin. Purity of monocytes was above 90%, as determined
109 by flow cytometry (FACScan; Becton Dickinson) using anti-CD3 (BD Biosciences)
110 and anti-CD14 (BD Biosciences) antibodies. SARS-CoV-2 (GenBank accession no.
111 MT710714) was expanded in Vero E6 cells. Viral isolation was performed after a
112 single passage in a cell culture in a 150 cm² flasks with high glucose DMEM plus
113 2% FBS. Observations for cytopathic effects were performed daily and peaked 4 to
114 5 days after infection. All procedures related to virus culture were handled in
115 biosafety level 3 (BSL3) multiuser facilities, according to WHO guidelines. Virus
116 titers were determined as plaque forming units (PFU/mL), and virus stocks were
117 kept in -80°C ultralow freezers. VIP and PACAP and the VPAC1 and VPAC2
118 agonists (Ala^{11,22,28})-VIP and Bay 55-9837, respectively, were purchased from
119 Tocris. The PAC1 agonist Maxadilan was kindly donated by Dr. Ethan A. Lerner
120 (Department of Dermatology, Massachusetts General Hospital, MA, USA). All
121 peptides and agonists were diluted in PBS. The inhibitors of the transcription factors
122 SREBP (AM580) and NF-KB (Bay 11-7082) were purchased from Selleckchem.

123 **Infections and virus titration.** Infections were performed with SARS-CoV-2 at MOI
124 of 0.01 (monocytes) or 0.1 (Calu-3) in low (monocytes) or high (Calu-3) glucose
125 DMEM without serum. After 1 hour, viral input was removed and cells were washed
126 and incubated with complete medium with treatments or not. For virus titration,
127 monolayers of Vero E6 cells (2×10^4 cell/well) in 96-well plates were infected with
128 serial dilutions of supernatants containing SARS-CoV-2 for 1 hour at 37°C. Semi-

129 solid high glucose DMEM medium containing 2% FBS and 2.4%
130 carboxymethylcellulose was added and cultures were incubated for 3 days at 37 °C.
131 Then, the cells were fixed with 10% formalin for 2 hours at room temperature. The
132 cell monolayer was stained with 0.04% solution of crystal violet in 20% ethanol for
133 1 hour. Plaque numbers were scored in at least 3 replicates per dilution by
134 independent readers blinded to the experimental group, and the virus titers were
135 determined by plaque-forming units (PFU) per milliliter.

136 **Molecular detection of virus RNA levels.** The total RNA was extracted from cells
137 using QIAamp Viral RNA (Qiagen), according to manufacturer's instructions.
138 Quantitative RT-PCR was performed using QuantiTect Probe RT-PCR Kit (Qiagen)
139 in a StepOnePlus™ Real-Time PCR System (Thermo Fisher Scientific).
140 Amplifications were carried out in 15 µL reaction mixtures containing 2x reaction
141 mix buffer, 50 µM of each primer, 10 µM of probe, and 5 µL of RNA template.
142 Primers, probes, and cycling conditions recommended by the Centers for Disease
143 Control and Prevention (CDC) protocol were used to detect the SARS-CoV-2 [33].
144 The standard curve method was employed for virus quantification. For reference to
145 the cell amounts used, the housekeeping gene RNase P was amplified. The Ct
146 values for this target were compared to those obtained to different cell amounts, 10⁷
147 to 10², for calibration.

148 **SDS-PAGE and Western blot for SREBPs.** After 24h of SARS-CoV-2 infection,
149 monocytes were harvested using ice-cold lysis buffer (1% Triton X-100, 2% SDS,
150 150 mM NaCl, 10 mM HEPES, 2 mM EDTA containing protease inhibitor cocktail -
151 Roche). Cell lysates were heated at 100 °C for 5 min in the presence of Laemmli
152 buffer (20% β-mercaptoethanol; 370 mM Tris base; 160 µM bromophenol blue; 6%

153 glycerol; 16% SDS; pH 6.8), and 20 µg of protein/sample were resolved by
154 electrophoresis on SDS-containing 10% polyacrylamide gel (SDS-PAGE). After
155 electrophoresis, the separated proteins were transferred to nitrocellulose
156 membranes and incubated in blocking buffer (5% nonfat milk, 50 mM Tris-HCl, 150
157 mM NaCl, and 0.1% Tween 20). Membranes were probed overnight with the
158 following antibodies: anti-SREBP-1 (Proteintech #14088-1-AP), anti-SREBP-2
159 (Proteintech #28212-1-AP) and anti-β-actin (Sigma, #A1978). After the washing
160 steps, they were incubated with IRDye - LICOR or HRP-conjugated secondary
161 antibodies. All antibodies were diluted in blocking buffer. The detections were
162 performed by Supersignal Chemiluminescence (GE Healthcare) or by fluorescence
163 imaging using the Odyssey system. Densitometries were analyzed using the Image
164 Studio Lite Version 5.2 software.

165 **Measurements of inflammatory mediators, cell death, NF-kBp65, CREB and**
166 **neuropeptides.** A multiplex biometric immunoassay containing fluorescent dyed
167 microbeads was used to measure cytokines in plasma samples (Bio-Rad
168 Laboratories). The following cytokines were quantified: Basic-FGF, CTRAK,
169 Eotaxin, G-CSF, GRO-α, HGF, IFN-α2, IFN-β, IFN-γ, IL-1α, IL-1β, IL-1RA, IL-2, IL-
170 2RA, IL-3, IL-4, IL-5, IL-6, IL-7, IL-8, IL-9, IP-10, IL-10, IL-12(p40), IL-13, IL-15, IL-
171 16, IL-17A, IL-18, LIF, M-CSF, MCP-3, MIF, MIG, MIP-1β, PDGF-BB, RANTES,
172 SCF, SCGF-1α, SCGF-β, TNFα, TNFβ, VEGF, β-NGF and PF4. Cytokine levels
173 were calculated by Luminex technology (Bio-Plex Workstation; Bio-Rad
174 Laboratories). The analysis of data was performed using software provided by the
175 manufacturer (Bio-Rad Laboratories). A range of 0.51–8000 pg/mL recombinant
176 cytokines was used to establish standard curves and the sensitivity of the assay.
177 The levels of IL-6, IL-8, TNF-α and MIF were quantified in the supernatants from

178 uninfected and SARS-CoV-2-infected Calu-3 cells and monocytes by ELISA (R&D
179 Systems), following manufacturer's instructions, and results are expressed as
180 percentages relative to uninfected cells. Cell death was determined according to the
181 activity of lactate dehydrogenase (LDH) in supernatants using CytoTox® Kit
182 (Promega) according to the manufacturer's instructions. Supernatants were
183 centrifuged at 5,000 rpm for 1 minute to remove cellular debris. Evaluation of NF-
184 kBp65 and CREB activation was performed in infected or uninfected monocytes
185 using NF-kB p65 (Total/Phospho) InstantOne™ and CREB (Total/Phospho)
186 Multispecies InstantOne™ ELISA Kits (Thermo Fisher), according to manufacturer's
187 instructions. VIP and PACAP levels were quantified in the plasma from patients or
188 control volunteers using standard commercially available ELISA and EIA Kits,
189 according to the manufacturer's instructions (Abelisa).

190 **Human subjects.** We prospectively enrolled patients with severe or
191 mild/asymptomatic COVID-19 RT-PCR-confirmed diagnosis, and SARS-CoV-2-
192 negative healthy controls. Blood and respiratory samples were obtained from 24
193 patients with severe COVID-19 within 72 hours from intensive care unit (ICU)
194 admission in two reference centers (Instituto Estadual do Cérebro Paulo Niemeyer
195 and Hospital Copa Star, Rio de Janeiro, Brazil). Severe COVID-19 was defined as
196 those critically ill patients presenting viral pneumonia on computed tomography scan
197 and requiring oxygen supplementation through either a nonrebreather mask or
198 mechanical ventilation. Eight outpatients presenting mild self-limiting COVID-19
199 syndrome, and two SARS-CoV-2-positive asymptomatic subjects were also
200 included. Patients had SARS-CoV-2 confirmed diagnostic through RT-PCR of nasal
201 swab or tracheal aspirates. Peripheral vein blood was also collected from 10 SARS-
202 CoV-2-negative healthy participants as tested by RT-PCR on the day of blood

203 sampling. Characteristics of severe (n=24), mild/asymptomatic (n=10) and healthy
204 (n=10) participants are presented in **Table 1**. Mild and severe COVID-19 patients
205 presented differences regarding age and presence of comorbidities, such as
206 obesity, cardiovascular diseases and diabetes (**Table 1**), which is consistent with
207 previously reported patient cohorts [2,34–36]. The SARS-CoV-2-negative control
208 group included subjects of older age and chronic non-communicable diseases, so it
209 is matched with mild and critical COVID-19 patients, except for hypertension (**Table**
210 **1**). All ICU-admitted patients received usual supportive care for severe COVID-19
211 and respiratory support with either noninvasive oxygen supplementation (n=5) or
212 mechanical ventilation (n=19) (**Supplemental Table 1**). Patients with acute
213 respiratory distress syndrome (ARDS) were managed with neuromuscular blockade
214 and a protective ventilation strategy that included low tidal volume (6 mL/kg of
215 predicted body weight) and limited driving pressure (less than 16 cmH₂O) as well
216 as optimal PEEP calculated based on the best lung compliance and PaO₂/FiO₂
217 ratio. In those patients with severe ARDS and PaO₂/FiO₂ ratio below 150 despite
218 optimal ventilatory settings, prone position was initiated. Our management protocol
219 included antithrombotic prophylaxis with enoxaparin 40 to 60 mg per day. Patients
220 did not receive routine steroids, antivirals or other anti-inflammatory or anti-platelet
221 drugs. The SARS-CoV-2-negative control participants were not under anti-
222 inflammatory or anti-platelet drugs for at least two weeks. All clinical information was
223 prospectively collected using a standardized form - ISARIC/WHO Clinical
224 Characterization Protocol for Severe Emerging Infections (CCPBR). Clinical and
225 laboratory data were recorded on admission in all severe patients included in the
226 study and the primary outcome analyzed was 28-day mortality (n = 11 survivors and
227 13 non-survivors, **Supplemental Table 2**). Age and frequency of comorbidities were

228 not different between severe patients requiring mechanical ventilation or
229 noninvasive oxygen supplementation neither between survivors and non-survivors
230 (**Supplemental Table 1 and 2**).

231 **Statistical analysis.** Statistics were performed using GraphPad Prism software
232 version 8. Numerical variables were tested regarding distribution using the Shapiro-
233 Wilk test. One-way analysis of variance (ANOVA) was used to compare differences
234 among 3 groups following a normal (parametric) distribution, and Tukey's post-hoc
235 test was used to locate the differences between the groups; or Friedman's test (for
236 non-parametric data) with Dunn's post-hoc test. Comparisons between 2 groups
237 were performed using the Student t test for parametric distributions or the Mann-
238 Whitney U test for nonparametric distributions. Correlation coefficients were
239 calculated using Pearson's correlation test for parametric distributions and the
240 Spearman's correlation test for nonparametric distributions.

241 **Results**

242 **Plasma levels of VIP are elevated in patients with severe forms of COVID-19**
243 **and associate with survival.** From April to May 2020, we followed up 24 critically
244 ill COVID-19 patients, at the median age of 53-year-old (**Table 1**), presenting the
245 most common infection symptoms and comorbidities, from whom we evaluated the
246 plasma levels of the neuropeptides VIP and PACAP, comparing with patients with
247 mild COVID-19 symptoms and non-infected healthy individuals. We found that
248 patients affected by the most severe forms of infection had higher plasma levels of
249 the neuropeptide VIP than uninfected healthy controls and asymptomatic/mild
250 patients (**Fig. 1A**). Comparing the viral load in positive swab samples from mild and
251 severe COVID-19 patients we found a modest positive correlation with VIP levels

252 **(Fig. 1B)**. Following, we examined a possible correlation between VIP levels of
253 severe patients and inflammatory markers. We identified that VIP negatively
254 correlated with five pro-inflammatory factors (IL-8, IL-12p40, IL-17A, TNF- α and
255 CXCL10/IP-10), and positively with two anti-inflammatory factors (IL-1RA and IL-10)
256 **(Fig. 1C-I)**. Next, severe COVID-19 patients were further subdivided between those
257 requiring invasive mechanical ventilation or noninvasive O₂ supplementation or
258 according to the 28-day mortality outcome as survivors or non-survivors. We did not
259 find a significant difference when analyzing O₂ supplementation versus mechanical
260 ventilation **(Fig. 1J)**, probably due to the low number of patients under the first
261 condition. On the contrary, we observed that VIP plasma levels associated with
262 survival of patients with severe COVID-19, being significantly higher in survivors
263 than in non-survivors **(Fig. 1K)**. For PACAP plasma levels, we did not find significant
264 differences between the groups analyzed, inflammatory markers, viral load or with
265 VIP levels (data not shown). The finding that survival of severe COVID-19 patients
266 is associated with higher levels of circulating VIP, a molecule with pro-homeostasis
267 and anti-inflammatory activities [32,37], moreover pointing to an application as a
268 prognostic marker, also implies to a therapeutical potential of VIP in COVID-19. In
269 fact, VIP has been approved for three clinical trials against COVID-19 in intravenous
270 [38] and inhaled [39,40] formulations. Our initial clinical data prompted us to
271 evaluate the effects of VIP (and of PACAP as well) on SARS-CoV-2-infected cells
272 to better corroborate the use of VIP as therapeutical agent in COVID-19 patients.

273 **VIP and PACAP reduce SARS-CoV-2 RNA synthesis in human primary**
274 **monocytes and viral replication in pulmonary cells, protecting them from**
275 **virus-mediated cytopathic effects.** Upon identifying the association of VIP with
276 survival of critical COVID-19 patients and considering that, in the setting of COVID-

277 19, the main affected cells are those present in the lung epithelium, including the
278 immune cells recruited upon infection, we sought to investigate the in vitro effects
279 of VIP and PACAP in SARS-CoV-2-infected cells. To this end, we initially evaluated
280 the SARS-CoV-2 RNA synthesis in monocytes (as the infection by SARS-CoV-2 in
281 this cell is non-productive [41,42]) and the viral replication in Calu-3 cells (a lineage
282 of lung epithelial cells highly susceptible to SARS-CoV-2) exposed to VIP or
283 PACAP). We found that VIP reduced the SARS-CoV-2 RNA synthesis in
284 monocytes, achieving up to 40% and 50% inhibition at 5 nM and 10 nM, respectively
285 (**Fig. 2A**). PACAP similarly decreased the levels of viral RNA synthesis with 5 nM
286 and 10 nM (up to 50% for both doses) (**Fig. 2B**). We next evaluated whether VIP
287 and PACAP could also be able to restrict virus production in pulmonary cells, one
288 of the major targets of SARS-CoV-2. We found that VIP reduced viral replication,
289 reaching up to 50% and 40% inhibition with 1 nM and 5 nM, respectively (**Fig. 2C**
290 **and Supp Fig. 1A**). PACAP also diminished virus production up to 40% and 50%
291 at concentrations equivalent to 10 nM and 50 nM (**Fig. 2D and Supp Fig. 1B**). In
292 parallel, VIP and PACAP protected monocytes and Calu-3 cells from SARS-CoV-2-
293 mediated cytopathic effect, as measured by LDH activity in supernatants (**Fig. 2E**
294 **and 2F**). Overall, these results show that cells exposed to VIP or PACAP present
295 decreased viral output and resistance to damages induced by the infection.

296 **Receptor contribution for the VIP and PACAP mediated inhibition of SARS-**
297 **CoV-2 replication.** The different optimal concentrations of VIP and PACAP to
298 reduce SARS-CoV-2 replication in Calu-3 cells might be explained by the relative
299 abundance of the neuropeptide receptors, since it has been shown that these cells
300 express only VPAC1 [43]. However, all three receptors are reported to be expressed
301 in lungs, with some studies showing that VPAC1 levels are higher than VPAC2 or

302 PAC1 (to which PACAP binds with higher affinity than to VPAC1 and VPAC2
303 [22,44–46]). With that in mind, we evaluated the role of the individual receptors in
304 the neuropeptide-mediated inhibition of SARS-CoV-2 in both cells. To this end,
305 monocytes were treated with specific agonists to VPAC1, VPAC2 and PAC1 (Ala-
306 VIP, Bay 55-9837 and Maxadilan, respectively), and then infected with SARS-CoV-
307 2. Activation of VPAC1 at 1 nM, 5 nM and 10 nM, and of VPAC2 at 1 nM, significantly
308 reduced the SARS-CoV-2 genome replication (**Fig. 3A**). We also verified that
309 VPAC1 is the main receptor involved the inhibition of SARS-CoV-2 in Calu-3 cells,
310 resembling the level of inhibition achieved with VIP, while the exposure to a VPAC2
311 agonist resulted in a more modest inhibition (**Fig. 3B**). The stimulus with a PAC1
312 agonist had no effect on viral replication (**Fig. 3A and 3B**). As a whole, these
313 findings suggest that VPAC1 receptor is the main contributor for the VIP- and
314 PACAP-mediated SARS-CoV-2 inhibition in monocytes and Calu-3 cells, and that
315 activation of this receptor can lead to a diminished viral replication similar to that
316 induced by the own neuropeptides.

317 **VIP and PACAP reduce the production of proinflammatory cytokines by**
318 **SARS-CoV-2-infected monocytes and Calu-3 cells.** Controlling the production of
319 proinflammatory cytokines may be critical for reducing SARS-CoV-2 replication and
320 limiting tissue damages, and based on evidence that VIP and PACAP can regulate
321 the inflammatory response [27,47], we next evaluated whether both neuropeptides
322 could attenuate the production of proinflammatory mediators by SARS-CoV-2-
323 infected monocytes or lung epithelial cells. As shown in **Fig. 4A**, SARS-CoV-2-
324 infected monocytes produced large amounts of the proinflammatory mediators IL-6,
325 IL-8, TNF and MIF relative to uninfected cells (15, 4, 12 and 18 times more,
326 respectively). In contrast, the treatment of SARS-CoV-2-infected monocytes with

327 either neuropeptide reduced to 66%, 50%, 66% and 50% the cellular production of
328 IL-6, IL-8, TNF and MIF, respectively. Furthermore, VIP and PACAP reverted by
329 approximately the same degree the release of IL-6 and IL-8 by Calu-3 cells (**Fig.**
330 **4B**), implying that VIP and PACAP may offer a critical protection to inflamed lungs
331 affected by SARS-CoV-2 replication. Because proinflammatory cytokines may favor
332 SARS-CoV-2 replication, which, in turn, can amplify the cellular synthesis of these
333 mediators, these findings may support our assumption that VIP and PACAP offer
334 tissue protection by inhibiting virus replication and regulating the boost of cytokine
335 production.

336 **VIP and PACAP regulate the activation of transcription factors in SARS-CoV-**
337 **2-infected monocytes.** Given that the transcription factor NF- κ B is critically
338 involved in the cellular production of inflammatory mediators [48], and our own
339 findings showing that VIP and PACAP can inhibit its activation in HIV-1-infected
340 macrophages [49], we investigated whether both neuropeptides would exert this
341 same effect on SARS-CoV-2-infected monocytes. We found that activated NF- κ B is
342 up-modulated in infected cells (as measured by the increased amount of
343 phosphorylated NF- κ Bp65 subunit), and that VIP and PACAP were able to reduce
344 NF- κ Bp65 phosphorylation (**Fig. 5A**). Following, we analyzed the effects of both
345 neuropeptides on the activation of CREB, a transcription factor induced by several
346 GPCR ligands, including VIP and PACAP [50], and also involved in the induction of
347 anti-inflammatory cytokines [51,52]. CREB and NF- κ B share the CREB-binding
348 protein/p300 (CBP/p300 protein) as a cofactor, and CREB activation results in the
349 inhibition of NF- κ B [53]. We found that activation of CREB was diminished in SARS-
350 CoV-2-infected monocytes (**Fig. 5B**), a result coherent with NF- κ B activation in the
351 same cells. Consistent with this finding, VIP and PACAP promoted CREB activation

352 (as measured by increase of CREB phosphorylation) in those infected monocytes,
353 a result matching the inhibition of NF- κ B and the reduction of cellular production of
354 proinflammatory cytokines. We also evaluated in SARS-CoV-2-infected monocytes
355 the expression of the active form of SREBP-1 and SREBP-2, transcription factors
356 that also interact with CBP/p300 [54], and are crucial for the replication of several
357 viruses, including coronaviruses [55–57]. In fact, we and other authors reported that
358 SARS-CoV-2 infection promotes the activation of SREBP, and that this activation is
359 associated with enhanced viral replication [58,59] and COVID-19 disease severity
360 [60]. We detected that the levels of both isoforms of SREBP in active state are
361 increased in SARS-CoV-2-infected monocytes and that VIP or PACAP treatment
362 prevented this augmentation, lowering them to the same basal levels found in
363 uninfected monocytes (**Fig. 5C and 5D, Supp. Fig. 2**).

364 **Inhibition of NF- κ B and SREBP in monocytes reduces SARS-CoV-2 RNA**
365 **synthesis, production of proinflammatory mediators and protects the cells**
366 **from virus-mediated cytopathic effects.** To directly connect these latter findings
367 with viral replication and production of pro-inflammatory mediators, we treated
368 SARS-CoV-2-infected monocytes with pharmacological inhibitors of NF- κ B (Bay
369 11-7082) or SREBP (AM580) [55,59], together or not with VIP and PACAP. We
370 found that the sole inhibition of SREBP decreased viral RNA synthesis and
371 production of TNF- α and IL-6, and reduced cell death, measurements that were all
372 amplified when the inhibitors were associated with either neuropeptide (Fig. 6, A-
373 D). Except for viral RNA synthesis, the sole inhibition of NF- κ B, or in combination
374 with VIP or PACAP, produced similar results (Fig. 6, A-D). Importantly, the
375 protecting effects mediated by VIP or PACAP alone were identical to those seen

376 when the signaling pathways triggered by NF-KB or SREBP activation were
377 specifically inhibited.

378 Together, our data suggest that the restriction of SARS-CoV-2 replication in
379 monocytes and in pulmonary cells by VIP and PACAP can be the outcome of the
380 intrinsic modulation of inflammatory mediators and transcription factors that are
381 involved directly and indirectly with the viral replication. Considering that VIP and
382 PACAP regulate inflammatory reactions, it is possible that their increased circulating
383 amounts reflect a counter-regulatory effect elicited by the dysregulated immune
384 response typical of the more severe clinical status of COVID-19 patients. Since
385 SARS-CoV-2-induced NF-kB and SREBP activation are key events involved in the
386 elevated production of proinflammatory cytokines in COVID-19 [58,60,61], the
387 inhibition of these transcription factors, associated with the reduction of
388 proinflammatory cytokines and with the decrease of viral replication by VIP and
389 PACAP, strengthen the potential of these neuropeptides as possible therapeutical
390 candidates for COVID-19.

391 **Discussion**

392 In this work, we identified that the plasma levels of the neuropeptide VIP are
393 elevated in patients with severe forms of COVID-19, correlating with viral load,
394 associated with reduced inflammation, and that the elevated VIP levels at ICU
395 admission predicted patients' favorable outcome, including association with patient
396 survival. In in vitro SARS-CoV-2-infected monocytes and epithelial lung cells, the
397 neuropeptides VIP and PACAP, endogenous molecules presenting anti-
398 inflammatory properties, reduced the exacerbated synthesis of proinflammatory
399 mediators, coupled with the inhibition of SARS-CoV-2 replication. Our findings

400 support and encourage clinical trials with VIP in COVID-19 patients, which are in
401 progress with intravenous [38] and inhaled [39,40] formulations and are expected to
402 be full disclosed this year and next. An initial release of the data, as preprint, shows
403 an increase in survival rates and reduction of IL-6 levels on those who received
404 intravenous Aviptadil (VIP) [62]. Our present data may substantiate additional larger
405 trials with VIP, an overlooked molecule associated with antiviral, anti-inflammatory
406 and enhanced survival activities.

407 Both neuropeptides regulate the inflammatory response due to their ability to
408 decrease the production of proinflammatory mediators, and to elicit the production
409 of anti-inflammatory molecules. Given that VIP and PACAP and their receptors are
410 systemically distributed, including lungs [22,63], brain, and gut, we believe that the
411 anti-SARS-CoV-2 effects of both neuropeptides would not be restricted to the
412 respiratory tract, as shown by many studies in other chronic inflammatory illnesses.

413 VIP and PACAP decreased SARS-CoV-2 genome replication in monocytes,
414 while protecting them from virus-induced cytopathicity. By diminishing the
415 intracellular levels of viral RNA and other viral molecules, VIP and PACAP could
416 prevent the cell death by pyroptosis, which has been described as one of the main
417 causes of cell damage during SARS-CoV-2 infection [13,14]. VIP and PACAP also
418 diminished the production of the proinflammatory cytokines IL-6, IL-8, TNF- α and
419 MIF by these cells, in agreement with the reported ability of these neuropeptides to
420 regulate the inflammatory response [24–27,64]. We found similar results with lung
421 epithelial cells, supporting that VIP and PACAP may offer a critical protection to
422 inflamed lungs affected by SARS-CoV-2 replication. It is possible that the higher

423 amounts of VIP in patients with severe forms of infection may reflect a counter-
424 regulatory feedback elicited by the dysregulated immune response of these patients.

425 We detected that the transcription factor CREB, which can act as a negative
426 regulator of NF- κ B [65,66], is down-regulated in SARS-CoV-2-infected monocytes,
427 in opposition to NF- κ B activation in the same cells, and that VIP and PACAP
428 reversed both phenomenon in infected monocytes. In some models [67–72], CREB
429 activation is related to induction of anti-inflammatory cytokines concomitant with
430 reduction of pro-inflammatory molecules and through competition with NF- κ B by
431 their shared co-activator protein CBP/p300 [51,65,66,72]. CREB activation is also
432 involved with the anti-apoptotic response in monocytes and macrophages, during
433 differentiation and inflammatory stimuli [73,74]. The imbalance between CREB and
434 NF- κ B, either as a direct effect of infection by SARS-CoV-2 or a consequence of
435 exposure of bystander cells to viral products and inflammatory molecules, could be
436 an important target for inhibition of SARS-CoV-2 deleterious effects, at least in
437 monocytes and probably also in lung cells, as a similar imbalance between CREB
438 and NF- κ B was observed in an acute inflammatory pulmonary condition [53].

439 Induction of SREBP activity by SARS-CoV-2 was consistent with data
440 showing its increase and association with COVID-19 severity in patients [60].
441 SREBP1 regulates the expression of genes of fatty acid biosynthesis, whilst
442 SREBP2 regulates genes involved in cholesterol biosynthesis, intracellular lipid
443 movement and lipoprotein import [75]. While crucial for metabolic homeostasis, both
444 transcription factors are involved in pathologies when misbalanced or overactivated
445 [75], and several viruses are reported to induce their activation, as the up-regulation
446 of host lipid biosynthesis is a requirement for their optimal replication [55–57]. As

447 reported by our group [58] and others authors [59], recently reported that SARS-
448 CoV-2 activates SREBP-1 and other pathways of lipid metabolism in human cells,
449 and that lipid droplets enhance viral replication and production of inflammatory
450 mediators. Similar to NF-kB and CREB, the association of SREBPs with CBP/p300
451 [54] makes its function susceptible to the availability of this co-factor, which
452 abundance can be low or high depending on the state of activation of NF-kB and
453 CREB. Thus, the modulation of each one of these factors by VIP and PACAP can
454 reflect a fine tuning of the transcriptional regulation of metabolic and inflammatory
455 pathways, which in turn can affect the replication of SARS-CoV-2. Our results with
456 inhibitors of SREBPs and NF-KB, used alone or in combination with either
457 neuropeptide, provide further connection between the ability of VIP and PACAP to
458 regulate the activity of these transcription factors and to control viral replication and
459 production of pro-inflammatory mediators, as well as to reduce SARS-CoV-2-
460 induced cell damages. The decline of viral genome replication and production of
461 inflammatory cytokines secondary to SREBP blockage are in agreement with
462 previous reports showing that this transcription factor is essential for replication of a
463 broad range of viruses, including coronaviruses in Calu-3 cells [55–57,59] and
464 contributes to cytokine storm in COVID-19 patients [60]. The diminished production
465 of TNF- α and IL-6 in our assays due to NF-KB inhibition agrees with its well-known
466 role to eliciting inflammatory responses. Overall, we believe that the protecting role
467 of VIP and PACAP against SARS-CoV-2 infection in vitro can be explained, at least
468 in part, by their ability to simultaneously regulate the signaling pathways elicited by
469 these transcription factors. Our findings are summarized in the model presented in
470 Fig. 7.

471 Because VIP and PACAP signaling outcome is dependent of the combined action
472 of the receptors activated by them (VIP and PACAP receptors can elicit cell
473 signaling in homo and hetero dimers; 72), we evaluated whether they were involved
474 in the final outcome analyzed. Our assays suggest that signaling through the
475 receptors VPAC1 and VPAC2 contributed for VIP- and PACAP-mediated reduction
476 of SARS-CoV-2 RNA synthesis in monocytes and viral production in Calu-3 cells,
477 with VPAC1 activation alone being able to reproduce the SARS-CoV-2 inhibition
478 promoted by the natural neuropeptides. The inhibition profile of SARS-CoV-2 by VIP
479 and PACAP in Calu-3 cells may be biased regarding the expected action in the
480 lungs, since Calu-3 cells appear to express only VPAC1 [43]. However, lung tissues,
481 while reported to express high levels of VPAC1, also express VPAC2 and PAC1
482 [44,46], and, more specifically, VPAC2 mRNA was detected in airway epithelial,
483 glandular, and immune cells of the lung [45]. Therefore, while the inhibition curve of
484 SARS-CoV-2 by VIP and PACAP in Calu-3 cells points to different optimal doses
485 than those obtained for monocytes, it is possible that in normal lung cells and tissue,
486 VIP and PACAP could present a broader range of action in the inhibition of SARS-
487 CoV-2. In fact, VIP and specific agonists for VPAC1 or VPAC2 have been proposed
488 and tested for respiratory conditions, such as asthma [77–79], pulmonary arterial
489 hypertension (PAH) [77,80,81] and chronic obstructive pulmonary disease (COPD)
490 [77,78,82], demonstrating that the anti-inflammatory actions of VIP and PACAP can
491 be achieved in lung tissues. Future studies should define which of these receptors
492 would preferentially be activated by specific agonists to restrain SARS-CoV-2
493 replication in lungs or other sites. Also, as G-coupled receptors ligands, it is
494 expected that VIP and PACAP curve profiles be subject to variation due receptor
495 density in cell, receptor isoforms, and subtypes of associated G proteins. Those

496 factors can influence the threshold and outcome of activation, and have been
497 described for a variety of G-coupled receptors, including VIP/PACAP receptors [83–
498 85]. Together with the possible differences of receptor expression and self-
499 regulatory characteristics of GPCRs, a third regulation level of VIP and PACAP
500 action on pulmonary cells can be achieved by the activity of proteases and
501 peptidases, as lungs are described to express high levels of several of them in both
502 normal and pathological conditions [86–88]. Some of these peptidases could target
503 VIP and PACAP, thus altering the ligand/receptor ratio and modulating the signaling
504 pathways.

505 Since our results were obtained with the pandemic SARS-CoV-2 D614G, we cannot
506 assure that the VIP and PACAP protective effects will also prevail against emerging
507 variants. Nonetheless, given that both neuropeptides regulate cellular mechanisms,
508 actions that might be independent of virus genotypes, we suppose that their
509 protective effects will likely be replicated against SARS-CoV-2 variants.

510 As up to now the availability of antivirals specific to SARS-CoV-2 is limited, and that
511 the hyper-inflammation may persist in COVID-19 patients even after the lowering of
512 the viral load, the searching for compounds that target the aberrant production of
513 proinflammatory cytokines and, simultaneously, the own viral replication, should be
514 stimulated. Our present results showing that VIP and PACAP hold these two critical
515 activities point these neuropeptides or their analogue molecules as potential
516 therapeutic agents for COVID-19.

517 **Acknowledgments**

518 We thank the Hemotherapy Service from Hospital Clementino Fraga Filho (Federal
519 University of Rio de Janeiro, Brazil) for providing buffy-coats. Dr. Andre Sampaio
520 from Farmanguinhos, platform RPT11M, and Dr. Lucio Mendes Cabral from
521 Department of Drugs and Pharmaceutics, Faculty of Pharmacy, Federal University
522 of Rio de Janeiro (UFRJ) are acknowledged for kindly donating the Calu-3 cell. The
523 recombinant protein Maxadilan was kindly donated to us by Dr. Ethan A. Lerner
524 (Department of Dermatology, Massachusetts General Hospital, MA, USA). The
525 authors are thankful to Prof. Elvira M. Saraiva (Federal University of Rio de Janeiro,
526 Brazil) for stimulating comments and invaluable suggestions. We pay tribute to Dr.
527 Juliana de Meis, our cherished young colleague who died prematurely, leaving a
528 significant legacy on knowledge of immunopathogenesis of parasitic diseases.

529 **Statement of Ethics**

530 Experimental procedures involving human cells from healthy donors were
531 performed with samples obtained after written informed consent and were approved
532 by the Institutional Review Board (IRB) of the Oswaldo Cruz Institute/Fiocruz (Rio
533 de Janeiro, RJ, Brazil) under the number 49971421.8.0000.5248. The National
534 Review Board approved the study protocol (CONEP 30650420.4.1001.0008) for
535 clinical samples, and informed consent was obtained from all participants or
536 patients' representatives.

537 **Conflict of Interest Statement**

538 The authors declare no competing financial interests.

539 **Funding**

540 This work was supported by Conselho Nacional de Desenvolvimento Científico e
541 Tecnológico (CNPq), Fundação de Amparo à Pesquisa do Estado do Rio de Janeiro
542 (FAPERJ), and by Mercosur Structural Convergence Fund (FOCEM, Mercosur,
543 grant number 03/11). This study was financed in part by the Coordenação de
544 Aperfeiçoamento de Pessoal de Nível Superior - Brasil (CAPES), Finance Code
545 001. Funding was also provided by CNPq, CAPES and FAPERJ through the
546 National Institutes of Science and Technology Program (INCT) to Carlos Morel
547 (INCT-IDPN) and Wilson Savino (INCT-NIM). Thanks are due to Oswaldo Cruz
548 Foundation/Fiocruz under the auspicious of Inova program. The funding sponsors
549 had no role in the design of the study; in the collection, analyses, or interpretation
550 of data; in the writing of the manuscript, and in the decision to publish the results.
551 The authors declare no competing financial interests.

552 **Author Contribution**

553 Conceived the study: JRT, TMLS, DCBH; Designed the experiments: JRT, PTB,
554 TMLS, DCBH; Performed the experiments: JRT, CQS, NFR, CRRP, CSF, SSGD,
555 ACF, MM, VCS, LT, IGAQ, EDH, PK; Analyzed the data: JRT, PTB, IGAQ, EDH,
556 PK, FAB, TMLS, DCBH; Wrote the paper: JRT, PTB, TMLS, DCBH. All authors
557 reviewed and approved the manuscript.

558 **References**

- 559 1 García LF. Immune Response, Inflammation, and the Clinical Spectrum of
560 COVID-19. *Front Immunol.* 2020 Jun;11:1441.
- 561 2 Huang C, Wang Y, Li X, Ren L, Zhao J, Hu Y, et al. Clinical features of
562 patients infected with 2019 novel coronavirus in Wuhan, China. *Lancet.*
563 2020 Feb;395(10223):497–506.
- 564 3 Chen G, Wu D, Guo W, Cao Y, Huang D, Wang H, et al. Clinical and
565 immunological features of severe and moderate coronavirus disease 2019. *J*

- 566 Clin Invest. 2020 Apr;130(5):2620–9.
- 567 4 Gupta A, Madhavan M V., Sehgal K, Nair N, Mahajan S, Sehrawat TS, et al.
568 Extrapulmonary manifestations of COVID-19. Nat Med. 2020
569 Jul;26(7):1017–32.
- 570 5 Tang D, Comish P, Kang R. The hallmarks of COVID-19 disease. PLoS
571 Pathog. 2020 May;16(5):e1008536.
- 572 6 Ragab D, Salah Eldin H, Taeimah M, Khattab R, Salem R. The COVID-19
573 Cytokine Storm; What We Know So Far. Front Immunol. 2020 Jun;11:1446.
- 574 7 Giamarellos-Bourboulis EJ, Netea MG, Rovina N, Akinosoglou K,
575 Antoniadou A, Antonakos N, et al. Complex Immune Dysregulation in
576 COVID-19 Patients with Severe Respiratory Failure. Cell Host Microbe.
577 2020 Jun;27(6):992-1000.e3.
- 578 8 Blanco-Melo D, Nilsson-Payant BE, Liu W-C, Uhl S, Hoagland D, Møller R,
579 et al. Imbalanced Host Response to SARS-CoV-2 Drives Development of
580 COVID-19. Cell. 2020 May;181(5):1036-1045.e9.
- 581 9 Veras FP, Pontelli MC, Silva CM, Toller-Kawahisa JE, de Lima M,
582 Nascimento DC, et al. SARS-CoV-2-triggered neutrophil extracellular traps
583 mediate COVID-19 pathology. J Exp Med. 2020 Dec;217(12):e20201129.
- 584 10 Radermecker C, Detrembleur N, Guiot J, Cavalier E, Henket M, D’Emal C,
585 et al. Neutrophil extracellular traps infiltrate the lung airway, interstitial, and
586 vascular compartments in severe COVID-19. J Exp Med. 2020
587 Dec;217(12):e20201012.
- 588 11 Skendros P, Mitsios A, Chrysanthopoulou A, Mastellos DC, Metallidis S,
589 Rafailidis P, et al. Complement and tissue factor–enriched neutrophil
590 extracellular traps are key drivers in COVID-19 immunothrombosis. J Clin
591 Invest. 2020 Nov;130(11):6151–7.
- 592 12 Middleton EA, He XY, Denorme F, Campbell RA, Ng D, Salvatore SP, et al.
593 Neutrophil extracellular traps contribute to immunothrombosis in COVID-19
594 acute respiratory distress syndrome. Blood. 2020 Sep;136(10):1169–79.
- 595 13 Rodrigues TS, de Sá KSG, Ishimoto AY, Becerra A, Oliveira S, Almeida L, et
596 al. Inflammasomes are activated in response to SARS-cov-2 infection and
597 are associated with COVID-19 severity in patients. J Exp Med. 2020
598 Mar;218(3):e20201707.
- 599 14 Ferreira AC, Soares VC, de Azevedo-Quintanilha IG, Dias S da SG,
600 Fintelman-Rodrigues N, Sacramento CQ, et al. SARS-CoV-2 engages
601 inflammasome and pyroptosis in human primary monocytes. Cell Death
602 Discov. 2021 Jun;7(1):43.
- 603 15 Nicholls JM, Poon LLM, Lee KC, Ng WF, Lai ST, Leung CY, et al. Lung
604 pathology of fatal severe acute respiratory syndrome. Lancet. 2003
605 May;361(9371):1773–8.
- 606 16 Gu J, Gong E, Zhang B, Zheng J, Gao Z, Zhong Y, et al. Multiple organ

- 607 infection and the pathogenesis of SARS. *J Exp Med.* 2005 Aug;202(3):415–
608 24.
- 609 17 Merad M, Martin JC. Pathological inflammation in patients with COVID-19: a
610 key role for monocytes and macrophages. *Nat Rev Immunol.* 2020
611 Jun;20(6):355–62.
- 612 18 Schurink B, Roos E, Radonic T, Barbe E, Bouman CSC, de Boer HH, et al.
613 Viral presence and immunopathology in patients with lethal COVID-19: a
614 prospective autopsy cohort study. *The Lancet Microbe.* 2020
615 Nov;1(7):e290–9.
- 616 19 Chiang C-C, Korinek M, Cheng W-J, Hwang T-L. Targeting Neutrophils to
617 Treat Acute Respiratory Distress Syndrome in Coronavirus Disease. *Front*
618 *Pharmacol.* 2020 Oct;11:1576.
- 619 20 Zhou J, Chu H, Li C, Wong BHY, Cheng ZS, Poon VKM, et al. Active
620 replication of middle east respiratory syndrome coronavirus and aberrant
621 induction of inflammatory cytokines and chemokines in human
622 macrophages: Implications for pathogenesis. *J Infect Dis.* 2014
623 Sep;209(9):1331–42.
- 624 21 Tynell J, Westenius V, Rönkkö E, Munster VJ, Melén K, Österlund P, et al.
625 Middle east respiratory syndrome coronavirus shows poor replication but
626 significant induction of antiviral responses in human monocyte-derived
627 macrophages and dendritic cells. *J Gen Virol.* 2016 Feb;97(2):344–55.
- 628 22 Dickson L, Finlayson K. VPAC and PAC receptors: From ligands to function.
629 *Pharmacol Ther.* 2009;121(3):294–316.
- 630 23 Ganea D, Delgado M. Vasoactive intestinal peptide (VIP) and pituitary
631 adenylate cyclase-activating polypeptide (PACAP) as modulators of both
632 innate and adaptive immunity. *Crit Rev Oral Biol Med.* 2002;13(3):229–37.
- 633 24 Kim WK, Kan Y, Ganea D, Hart RP, Gozes I, Jonakait GM. Vasoactive
634 intestinal peptide and pituitary adenylyl cyclase-activating polypeptide inhibit
635 tumor necrosis factor- α production in injured spinal cord and in activated
636 microglia via a cAMP-dependent pathway. *J Neurosci.* 2000
637 May;20(10):3622–30.
- 638 25 Larocca L, Calafat M, Roca V, Franchi AM, Leiros CP. VIP limits LPS-
639 induced nitric oxide production through IL-10 in NOD mice. *Int*
640 *Immunopharmacol.* 2007;7(10):1343–9.
- 641 26 Gonzalez-Rey E, Delgado M. Vasoactive intestinal peptide inhibits
642 cyclooxygenase-2 expression in activated macrophages, microglia, and
643 dendritic cells. *Brain Behav Immun.* 2008 Jan;22(1):35–41.
- 644 27 Delgado M, Munoz-Elias EJ, Gomariz RP, Ganea D. VIP and PACAP inhibit
645 IL-12 production in LPS-stimulated macrophages. Subsequent effect on
646 IFN γ synthesis by T cells. *J Neuroimmunol.* 1999 May;96(2):167–81.
- 647 28 Delgado M, Munoz-Elias EJ, Gomariz RP, Ganea D. Vasoactive intestinal
648 peptide and pituitary adenylate cyclase-activating polypeptide prevent

- 649 inducible nitric oxide synthase transcription in macrophages by inhibiting NF-
650 kappa B and IFN regulatory factor 1 activation. *J Immunol.* 1999
651 Apr;162(8):4685–96.
- 652 29 Moody TW, Ito T, Osefo N, Jensen RT. VIP and PACAP: recent insights into
653 their functions/roles in physiology and disease from molecular and genetic
654 studies. *Curr Opin Endocrinol Diabetes Obes.* 2011;18(1):61–7.
- 655 30 Gonzalez-Rey E, Varela N, Chorny A, Delgado M. Therapeutical
656 Approaches of Vasoactive Intestinal Peptide as a Pleiotropic
657 Immunomodulator. *Curr Pharm Des.* 2007 Apr;13(11):1113–39.
- 658 31 Pozo D, Gonzalez-Rey E, Chorny A, Anderson P, Varela N, Delgado M.
659 Tuning immune tolerance with vasoactive intestinal peptide: A new
660 therapeutic approach for immune disorders. *Peptides.* 2007
661 Sep;28(9):1833–46.
- 662 32 Martínez C, Juarranz Y, Gutiérrez-Cañas I, Carrión M, Pérez-García S,
663 Villanueva-Romero R, et al. A Clinical Approach for the Use of VIP Axis in
664 Inflammatory and Autoimmune Diseases. *Int J Mol Sci.* 2019 Dec;21(1):65.
- 665 33 CDC. Real-time RT-PCR Primers and Probes for COVID-19 [Internet].
666 Centers Dis Control Prev. 2020 [cited 2020 Dec 4]. Available from:
667 [https://www.cdc.gov/coronavirus/2019-ncov/lab/rt-pcr-panel-primer-](https://www.cdc.gov/coronavirus/2019-ncov/lab/rt-pcr-panel-primer-probes.html)
668 [probes.html](https://www.cdc.gov/coronavirus/2019-ncov/lab/rt-pcr-panel-primer-probes.html)
- 669 34 Wu C, Chen X, Cai Y, Xia J, Zhou X, Xu S, et al. Risk Factors Associated
670 With Acute Respiratory Distress Syndrome and Death in Patients With
671 Coronavirus Disease 2019 Pneumonia in Wuhan, China. *JAMA Intern Med.*
672 2020 Jul;180(7):934.
- 673 35 Shi S, Qin M, Shen B, Cai Y, Liu T, Yang F, et al. Association of Cardiac
674 Injury With Mortality in Hospitalized Patients With COVID-19 in Wuhan,
675 China. *JAMA Cardiol.* 2020 Jul;5(7):802.
- 676 36 Guo T, Fan Y, Chen M, Wu X, Zhang L, He T, et al. Cardiovascular
677 Implications of Fatal Outcomes of Patients With Coronavirus Disease 2019
678 (COVID-19). *JAMA Cardiol.* 2020 Jul;5(7):811.
- 679 37 Souza-Moreira L, Campos-Salinas J, Caro M, Gonzalez-Rey E.
680 Neuropeptides as pleiotropic modulators of the immune response.
681 *Neuroendocrinology.* 2011;94(2):89–100.
- 682 38 NCT0431169. Intravenous Aviptadil for Critical COVID-19 With Respiratory
683 Failure [Internet]. [ClinicalTrials.gov] Bethesda Natl Libr Med (US). [cited
684 2020 Jul 21]. Available from: <https://clinicaltrials.gov/ct2/show/NCT04311697>
- 685 39 NCT04536350. Inhaled Aviptadil for the Treatment of Moderate and Severe
686 COVID-19 [Internet]. [ClinicalTrials.gov] Bethesda Natl Libr Med (US). [cited
687 2020 Jul 25]. Available from: <https://clinicaltrials.gov/ct2/show/NCT04360096>
- 688 40 NCT04844580. A Clinical Study Evaluating Inhaled Aviptadil on COVID-19
689 [Internet]. [ClinicalTrials.gov] Bethesda Natl Libr Med (US). [cited 2021 Jul
690 1]. Available from: <https://clinicaltrials.gov/ct2/show/NCT04844580>

- 691 41 Boumaza A, Gay L, Mezouar S, Bestion E, Diallo AB, Michel M, et al.
692 Monocytes and macrophages, targets of severe acute respiratory syndrome
693 coronavirus 2: The clue for coronavirus disease 2019 immunoparalysis. *J*
694 *Infect Dis.* 2021 Aug;224(3):395–406.
- 695 42 Zheng J, Wang Y, Li K, Meyerholz DK, Allamargot C, Perlman S. Severe
696 Acute Respiratory Syndrome Coronavirus 2-Induced Immune Activation and
697 Death of Monocyte-Derived Human Macrophages and Dendritic Cells. *J*
698 *Infect Dis.* 2021 Mar;223(5):785–95.
- 699 43 Dérand R, Montoni A, Bulteau-Pignoux L, Janet T, Moreau B, Muller JM, et
700 al. Activation of VPAC 1 receptors by VIP and PACAP-27 in human
701 bronchial epithelial cells induces CFTR-dependent chloride secretion. *Br J*
702 *Pharmacol.* 2004 Feb;141(4):698–708.
- 703 44 Busto R, Prieto JC, Bodega G, Zapatero J, Carrero I. Immunohistochemical
704 localization and distribution of VIP/PACAP receptors in human lung.
705 *Peptides.* 2000 Feb;21(2):265–9.
- 706 45 Groneberg DA, Hartmann P, Dinh QT, Fischer A. Expression and
707 distribution of vasoactive intestinal polypeptide receptor VPAC2 mRNA in
708 human airways. *Lab Investig.* 2001;81(5):749–55.
- 709 46 Fagerberg L, Hallstrom BM, Oksvold P, Kampf C, Djureinovic D, Odeberg J,
710 et al. Analysis of the human tissue-specific expression by genome-wide
711 integration of transcriptomics and antibody-based proteomics. *Mol Cell*
712 *Proteomics.* 2014 Feb;13(2):397–406.
- 713 47 Delgado M, Garrido E, Martinez C, Leceta J, Gomariz RP. Vasoactive
714 intestinal peptide and pituitary adenylate cyclase-activating polypeptides
715 (PACAP27) and PACAP38) protect CD4+CD8+ thymocytes from
716 glucocorticoid-induced apoptosis. *Blood.* 1996;87(12):5152–61.
- 717 48 Liu T, Zhang L, Joo D, Sun S-C. NF- κ B signaling in inflammation. *Signal*
718 *Transduct Target Ther.* 2017 Dec;2(1):17023.
- 719 49 Temerozo JR, de Azevedo SSD, Insuela DBR, Vieira RC, Ferreira PLC,
720 Carvalho VF, et al. The Neuropeptides Vasoactive Intestinal Peptide and
721 Pituitary Adenylate Cyclase-Activating Polypeptide Control HIV-1 Infection in
722 Macrophages Through Activation of Protein Kinases A and C. *Front*
723 *Immunol.* 2018 Jun;9(JUN):1336.
- 724 50 Schomerus C, Maronde E, Laedtke E, Korf HW. Vasoactive intestinal
725 peptide (VIP) and pituitary adenylate cyclase-activating polypeptide
726 (PACAP) induce phosphorylation of the transcription factor CREB in
727 subpopulations of rat pinealocytes: immunocytochemical and
728 immunochemical evidence. *Cell Tissue Res.* 1996;286(3):305–13.
- 729 51 Matt T. Transcriptional control of the inflammatory response: a role for the
730 CREB-binding protein (CBP). *Acta Med Austriaca.* 2002;29(3):77–9.
- 731 52 Wen AY, Sakamoto KM, Miller LS. The Role of the Transcription Factor
732 CREB in Immune Function. *J Immunol.* 2010 Dec;185(11):6413–9.

- 733 53 Shenkar R, Yum H-K, Arcaroli J, Kupfner J, Abraham E. Interactions
734 between CBP, NF- κ B, and CREB in the lungs after hemorrhage and
735 endotoxemia. *Am J Physiol Cell Mol Physiol*. 2001 Aug;281(2):L418–26.
- 736 54 Toth JI, Datta S, Athanikar JN, Freedman LP, Osborne TF. Selective
737 Coactivator Interactions in Gene Activation by SREBP-1a and -1c. *Mol Cell*
738 *Biol*. 2004 Sep;24(18):8288–300.
- 739 55 Yuan S, Chu H, Chan JF-W, Ye Z-W, Wen L, Yan B, et al. SREBP-
740 dependent lipidomic reprogramming as a broad-spectrum antiviral target.
741 *Nat Commun*. 2019 Dec;10(1):120.
- 742 56 Cloherty APM, Olmstead AD, Ribeiro CMS, Jean F. Hijacking of Lipid
743 Droplets by Hepatitis C, Dengue and Zika Viruses—From Viral Protein
744 Moonlighting to Extracellular Release. *Int J Mol Sci*. 2020 Oct;21(21):7901.
- 745 57 Taylor HE, Linde ME, Khatua AK, Popik W, Hildreth JEK. Sterol Regulatory
746 Element-Binding Protein 2 Couples HIV-1 Transcription to Cholesterol
747 Homeostasis and T Cell Activation. *J Virol*. 2011 Aug;85(15):7699–709.
- 748 58 Dias S da SG, Soares VC, Ferreira AC, Sacramento CQ, Fintelman-
749 Rodrigues N, Temerozo JR, et al. Lipid droplets fuel SARS-CoV-2
750 replication and production of inflammatory mediators. *PLOS Pathog*. 2020
751 Dec;16(12):e1009127.
- 752 59 Zhang S, Wang J, Cheng G. Protease cleavage of RNF20 facilitates
753 coronavirus replication via stabilization of SREBP1. *Proc Natl Acad Sci U S*
754 *A*. 2021 Sep;118(37). DOI: 10.1073/pnas.2107108118
- 755 60 Lee W, Ahn JH, Park HH, Kim HN, Kim H, Yoo Y, et al. COVID-19-activated
756 SREBP2 disturbs cholesterol biosynthesis and leads to cytokine storm.
757 *Signal Transduct Target Ther*. 2020 Dec;5(1):186.
- 758 61 Kircheis R, Haasbach E, Lueftenegger D, Heyken WT, Ocker M, Planz O.
759 NF- κ B Pathway as a Potential Target for Treatment of Critical Stage COVID-
760 19 Patients. *Front Immunol*. 2020 Dec;11:3446.
- 761 62 Youssef JG, Lee R, Javitt J, Lavin P, Lenhardt R, Park DJ, et al. Increased
762 Recovery and Survival in Patients With COVID-19 Respiratory Failure
763 Following Treatment with Aviptadil: Report #1 of the ZYESAMI COVID-19
764 Research Group. *SSRN Electron J*. 2021 Aug DOI: 10.2139/ssrn.3830051
- 765 63 Said SI. The discovery of VIP: Initially looked for in the lung, isolated from
766 intestine, and identified as a neuropeptide. *Peptides*. 2007 Sep;28(9):1620–
767 1.
- 768 64 Delgado M, Munoz-Elias EJ, Martinez C, Gomariz RP, Ganea D. VIP and
769 PACAP38 modulate cytokine and nitric oxide production in peritoneal. *Ann N*
770 *Y Acad Sci*. 1999;897:401–14.
- 771 65 Parry GC, Mackman N. Role of cyclic AMP response element-binding
772 protein in cyclic AMP inhibition of NF- κ B-mediated transcription. *J*
773 *Immunol*. 1997 Dec;159(11):5450–6.

- 774 66 Ollivier V, Parry GCN, Cobb RR, de Prost D, Mackman N. Elevated Cyclic
775 AMP Inhibits NF- κ B-mediated Transcription in Human Monocytic Cells and
776 Endothelial Cells. *J Biol Chem*. 1996 Aug;271(34):20828–35.
- 777 67 Luan B, Yoon YS, Lay J Le, Kaestner KH, Hedrick S, Montminy M. CREB
778 pathway links PGE2 signaling with macrophage polarization. *Proc Natl Acad
779 Sci U S A*. 2015 Dec;112(51):15642–7.
- 780 68 Zhao L. Suppression of Proinflammatory Cytokines Interleukin-1 and Tumor
781 Necrosis Factor- in Astrocytes by a V1 Vasopressin Receptor Agonist: A
782 cAMP Response Element-Binding Protein-Dependent Mechanism. *J
783 Neurosci*. 2004 Mar;24(9):2226–35.
- 784 69 Morris RHK, Tonks AJ, Jones KP, Ahluwalia MK, Thomas AW, Tonks A, et
785 al. DPPC regulates COX-2 expression in monocytes via phosphorylation of
786 CREB. *Biochem Biophys Res Commun*. 2008 May;370(1):174–8.
- 787 70 Ernst O, Glucksam-Galnoy Y, Bhatta B, Athamna M, Ben-Dror I, Glick Y, et
788 al. Exclusive Temporal Stimulation of IL-10 Expression in LPS-Stimulated
789 Mouse Macrophages by cAMP Inducers and Type I Interferons. *Front
790 Immunol*. 2019 Aug;10:1788.
- 791 71 Barátki BL, Huber K, Sármay G, Matkó J, Kövesdi D. Inflammatory signal
792 induced IL-10 production of marginal zone B-cells depends on CREB.
793 *Immunol Lett*. 2019 Aug;212:14–21.
- 794 72 Avni D, Ernst O, Philosoph A, Zor T. Role of CREB in modulation of TNF α
795 and IL-10 expression in LPS-stimulated RAW264.7 macrophages. *Mol
796 Immunol*. 2010 Apr;47(7–8):1396–403.
- 797 73 Park JM, Greten FR, Wong A, Westrick RJ, Arthur JSC, Otsu K, et al.
798 Signaling Pathways and Genes that Inhibit Pathogen-Induced Macrophage
799 Apoptosis— CREB and NF- κ B as Key Regulators. *Immunity*. 2005
800 Sep;23(3):319–29.
- 801 74 Cheng JC, Kinjo K, Judelson DR, Chang J, Wu WS, Schmid I, et al. CREB is
802 a critical regulator of normal hematopoiesis and leukemogenesis. *Blood*.
803 2008 Feb;111(3):1182–92.
- 804 75 Shimano H, Sato R. SREBP-regulated lipid metabolism: convergent
805 physiology — divergent pathophysiology. *Nat Rev Endocrinol*. 2017
806 Dec;13(12):710–30.
- 807 76 Harikumar KG, Morfis MM, Lisenbee CS, Sexton PM, Miller LJ. Constitutive
808 formation of oligomeric complexes between family B G protein-coupled
809 vasoactive intestinal polypeptide and secretin receptors. *Mol Pharmacol*.
810 2006;69(1):363–73.
- 811 77 Wu D, Lee D, Sung YK. Prospect of vasoactive intestinal peptide therapy for
812 COPD/PAH and asthma: a review. *Respir Res*. 2011 Dec;12(1):45.
- 813 78 Onoue S, Yamada S, Yajima T. Bioactive analogues and drug delivery
814 systems of vasoactive intestinal peptide (VIP) for the treatment of
815 asthma/COPD. *Peptides*. 2007 Sep;28(9):1640–50.

- 816 79 Lindén A, Hansson L, Andersson A, Palmqvist M, Arvidsson P, Löfdahl CG,
817 et al. Bronchodilation by an inhaled VPAC2 receptor agonist in patients with
818 stable asthma. *Thorax*. 2003 Mar;58(3):217–21.
- 819 80 Hamidi SA, Lin RZ, Szema AM, Lyubsky S, Jiang YP, Said SI. VIP and
820 endothelin receptor antagonist: An effective combination against
821 experimental pulmonary arterial hypertension. *Respir Res*. 2011
822 Dec;12(1):141.
- 823 81 Hilaire RC, Murthya SN, Kadowitza PJ, Jeter JR. Role of VPAC1 and
824 VPAC2 in VIP mediated inhibition of rat pulmonary artery and aortic smooth
825 muscle cell proliferation. *Peptides*. 2010;31(8):1517–22.
- 826 82 Burian B, Angela S, Nadler B, Petkov V, Block LH. Inhaled Vasoactive
827 Intestinal Peptide (VIP) improves the 6-minute walk test and quality of life in
828 patients with COPD: The VIP/COPD-trial. *Chest*. 2006 Oct;130(4):121S.
- 829 83 Couvineau A, Laburthe M. VPAC receptors: structure, molecular
830 pharmacology and interaction with accessory. *Br J Pharmacol*. 2012
831 May;166(1):42–50.
- 832 84 Gurevich V V., Gurevich E V. Biased GPCR signaling: Possible mechanisms
833 and inherent limitations. *Pharmacol Ther*. 2020;211. DOI:
834 10.1016/j.pharmthera.2020.107540
- 835 85 Gether U. Uncovering molecular mechanisms involved in activation of G
836 protein-coupled. *Endocr Rev*. 2000;21(1):90–113.
- 837 86 Van Der Velden VHJ, Wierenga-Wolf AF, Adriaansen-Soeting PWC,
838 Overbeek SE, Möller GM, Hoogsteden HC, et al. Expression of
839 aminopeptidase N and dipeptidyl peptidase IV in the healthy and asthmatic
840 bronchus. *Clin Exp Allergy*. 1998;28(1):110–20.
- 841 87 Dreytmueller D, Uhlig S, Ludwig A. ADAM-family metalloproteinases in lung
842 inflammation: potential therapeutic targets. *Am J Physiol Cell Mol Physiol*.
843 2015 Feb;308(4):L325–43.
- 844 88 Bonda WLM, Iochmann S, Magnen M, Courty Y, Reverdiau P. Kallikrein-
845 related peptidases in lung diseases. *Biol Chem*. 2018 Sep;399(9):959–71.
- 846
- 847

848 **Figure legends**

849 **Figure 1. Plasma levels of VIP are elevated in patients with severe forms of**
850 **COVID-19 and associates with reduced levels of inflammatory markers and**
851 **with survival.** The levels of VIP (**A**) in the plasma of SARS-CoV-2-negative control
852 participants, SARS-CoV-2-positive asymptomatic subjects, or symptomatic patients
853 presenting mild to severe COVID-19 were quantified by ELISA. Correlation between
854 levels of VIP and viral load (**B**) or inflammation markers (**C-I**). Severe COVID-19
855 patients admitted to the ICU were sub-divided between those requiring invasive
856 mechanical ventilation or noninvasive O₂ supplementation (**J**) and according to the
857 28-day mortality outcome as survivors or non survivors (**K**). Linear regression (with
858 the 95% confidence interval) and Spearman's correlation were calculated according
859 to the distribution of the data. Dots represent: Controls, grey; Asymptomatics, blue;
860 Mild, brown; Severe, red). The horizontal lines in the box plots represent the median,
861 the box edges represent the interquartile ranges, and the whiskers indicate the
862 minimal and maximal value in each group. * $p \leq .05$; ** $p \leq .01$.

863 **Figure 2. VIP and PACAP reduce SARS-CoV-2 RNA synthesis in human**
864 **primary monocytes and viral replication in pulmonary cells, protecting them**
865 **from virus-mediated cytopathic effects.** Monocytes (**A, B**) and Calu-3 cells (**C,**
866 **D**) were exposed (overnight) or not to the indicated concentrations of VIP (**A, C**) or
867 PACAP (**B, D**). Culture medium was removed and then cells were infected with
868 SARS-CoV-2. After infection, viral input was removed and cells were washed, then
869 re-exposed to the neuropeptides. Viral RNA synthesis was evaluated by qPCR in
870 monocytes 24 hours after infection. In Calu-3 cells, supernatants were collected at
871 48 hours after infection, and viral replication was evaluated by quantifying PFUs in

872 Vero E6 plaque assays. Cellular viability was analyzed by measuring LDH release
873 in the supernatants of uninfected or SARS-CoV-2-infected monocytes (**E**) treated or
874 not with VIP or PACAP (10 nM), and Calu-3 cells (**F**) treated or not with VIP (1 nM)
875 or PACAP (50 nM). Data in (**A, B**) are shown normalized to infected cells kept only
876 with culture medium, and in (**C, D, E, F**) represent means \pm SD of absolute values.
877 * $p \leq .05$; ** $p \leq .01$; (A, B, E) $n=6$; (C, D, F) $n=5$. Each dot represents an independent
878 assay with three replicates.

879 **Figure 3. Receptor contribution for the VIP and PACAP mediated inhibition of**
880 **SARS-CoV-2 replication.** Monocytes (**A**) and Calu-3 cells (**B**) were treated
881 (overnight) or not with agonists for VIP and PACAP receptors, as indicated, at
882 different concentrations. Culture medium was removed and then cells were infected
883 with SARS-CoV-2. After infection, viral input was removed, and cells were washed,
884 and then re-exposed to the receptor agonists. Viral RNA synthesis was evaluated
885 by qPCR in monocytes 24 hours after infection. In Calu-3 cells, supernatants were
886 collected at 48 hours after infection, and viral replication was evaluated by
887 quantifying PFUs in Vero E6 plaque assays. Data in (**A**) are shown normalized to
888 infected cells kept only with culture medium, and in (**B**) represents means \pm SD of
889 absolute values. * $p \leq .05$; ** $p \leq .01$; *** $p \leq .001$; (A, B) $n=4$. Each dot represents an
890 independent assay with three replicates.

891 **Figure 4. VIP and PACAP reduce the production of proinflammatory mediators**
892 **by SARS-CoV-2-infected monocytes and Calu-3 cells.** Monocytes (**A**) and Calu-
893 3 cells (**B**) were treated (overnight) or not with VIP or PACAP (10 nM each for
894 monocytes, 1 nM of VIP or 50 nM of PACAP for Calu-3 cells). Culture medium was
895 removed and then cells were infected with SARS-CoV-2. After infection, viral input

896 was removed and cells were washed, and then re-exposed to the neuropeptides.
897 The levels of IL-6, IL-8, TNF- α and MIF were measured in culture supernatants of
898 monocytes after 24 hours (**A**), and of IL-6 and IL-8 after 48 hours for Calu-3 cells
899 (**B**), by ELISA. Data represent means \pm SD. * $p \leq .05$; ** $p \leq .01$; (A) n=6; (B) n=4.
900 Each dot represents an independent assay with three replicates.

901 **Figure 5. VIP and PACAP regulate the activation of transcription factors in**
902 **SARS-CoV-2-infected monocytes.** Monocytes were treated (overnight) or not with
903 to VIP or PACAP (10 nM), culture medium was removed and then cells were infected
904 with SARS-CoV-2. After infection, viral input was removed, and cells were washed
905 and then re-exposed to the neuropeptides. After 24 hours, cells were lysed and the
906 ratios between phosphoNF-kBp65 and total NF-kBp65 (**A**), phosphoCREB and total
907 CREB (**B**), active SREBP-1 and β -actin (**C**), and active SREBP-2 and β -actin (**D**)
908 were quantified by ELISA (**A, B**) or by western blot (**C, D**) in the cell lysates. Data
909 represent means \pm SD. * $p \leq .05$; ** $p \leq .01$; *** $p \leq .001$; (A, B) n=3; (C, D) n=4. Each
910 dot represents an independent assay with three replicates.

911 **Figure 6. Inhibition of NF-kB and SREBP in monocytes reduces SARS-CoV-2**
912 **RNA synthesis, production of proinflammatory mediators and protects the**
913 **cells from virus-mediated cytopathic effects.** Monocytes were treated
914 (overnight) or not with to VIP or PACAP (5 nM), culture medium was removed and
915 then cells were infected with SARS-CoV-2. After infection, viral input was removed,
916 and cells were washed and then re-exposed to the neuropeptides associated or not
917 with inhibitors of SREBP (AM580, 10 μ M) or NF-kB (Bay 11-7082, 10 μ M). Viral
918 RNA synthesis (**A**), cellular viability (**B**) and levels of TNF- α and IL-6 (**C, D**) were
919 evaluated by qPCR, ELISA and LDH release, respectively, in the culture

920 supernatants 24 hours after infection. Data in (A) are shown normalized to infected
 921 cells kept only with culture medium, and in (B, C, D) represent means \pm SD of
 922 absolute values. * $p \leq .05$; ** $p \leq .01$; *** $p \leq .001$; (A - D) $n=6$. Each dot represents an
 923 independent assay with three replicates.

924 **Figure 7. Graphical summary of study data.** In severe COVID-19 patients, VIP
 925 plasma levels correlated with decreased inflammatory markers and survival. In in
 926 vitro assays with monocytes and lung epithelial cells, VIP and PACAP were found
 927 to decrease SARS-CoV-2 RNA synthesis (monocytes) and viral replication (lung
 928 epithelial cells). Both neuropeptides also reduced inflammatory factors and cell
 929 death of infected cells. Created with BioRender.com

930 **Table 1:** Characteristics of COVID-19 patients and control subjects.

Characteristics ¹	Control (n=10)	Asymptomatic/ Mild (n=10)	Severe/critical (n=24)
Age, years	53 (32 – 60)	43 (24 – 52)	58 (48 – 66)
Sex, male	4 (40%)	4 (40%)	12 (50%)
Respiratory support			
Oxygen supplementation	0 (0%)	0 (0%)	5 (20.8%)
Mechanical ventilation	0 (0%)	0 (0%)	19 (79.2%)
SAPS 3	-	-	60 (55 – 71)
PaO ₂ /FiO ₂ ratio	-	-	154 (99 – 373)
Vasopressor	-	-	10 (41.6%)
Time from symptom onset to blood sample, days	-	6 (-1 – 8) ²	14 (8 – 17)
28-day mortality	-	-	13 (54.2%)
Comorbidities			
Obesity	1 (10%)	1 (10%)	5 (20.8%)
Hypertension	1 (10%)	2 (20%)	6 (25%)
Diabetes	0 (0%)	0 (0%)	9 (37.5%)
Cancer	0 (0%)	0 (0%)	3 (12.5%)
Heart disease ³	0 (0%)	0 (0%)	2 (8.3%)
Presenting symptoms			
Cough	0 (0%)	3 (30%)	17 (70.8%)
Fever	0 (0%)	5 (50%)	18 (75%)
Dyspnea	0 (0%)	0 (0%)	20 (83.3%)
Headache	0 (0%)	4 (40%)	3 (12.5%)

Anosmia	0 (0%)	4 (40%)	8 (33.3%)
Laboratory findings on admission			
Leukocytes, x 1000/ μ L	-	-	138 (102 – 180)
Lymphocyte, cells/ μ L	-	-	1,167 (645 – 1,590)
Monocytes, cells/ μ L	-	-	679 (509 – 847)
Platelet count, x 1000/ μ L	-	-	169 (137 – 218)
C Reactive Protein, mg/L ⁴	0.1 (0.1 – 0.18)	0.2 (0.1 – 0.13)	178 (74 – 308)*
Fibrinogen, mg/dL ⁴	281 (232 – 302)	248 (182 – 341)	528 (366 – 714)*
D-dimer, IU/mL ⁴	292 (225 – 476)	191 (187 – 313)	4836 (2364 – 10816)*

931 ¹Numerical variables are represented as the median and the interquartile range, and
 932 qualitative variables are represented as the number and the percentage.

933 ²Day of sample collection after the onset of symptoms was not computed for asymptomatic
 934 subjects.

935 ³Coronary artery disease or congestive heart failure.

936 ⁴Reference values of C reactive Protein (0.00 – 1.00), Fibrinogen (238 – 498 mg/dL) and
 937 D-dimer (0 – 500 ng/mL).

938 *p < 0.05 compared to control. The qualitative variables were compared using the two tailed
 939 Fisher exact test, and the numerical variables using the t test for parametric and the Mann
 940 Whitney U test for nonparametric distributions.

Figure 1

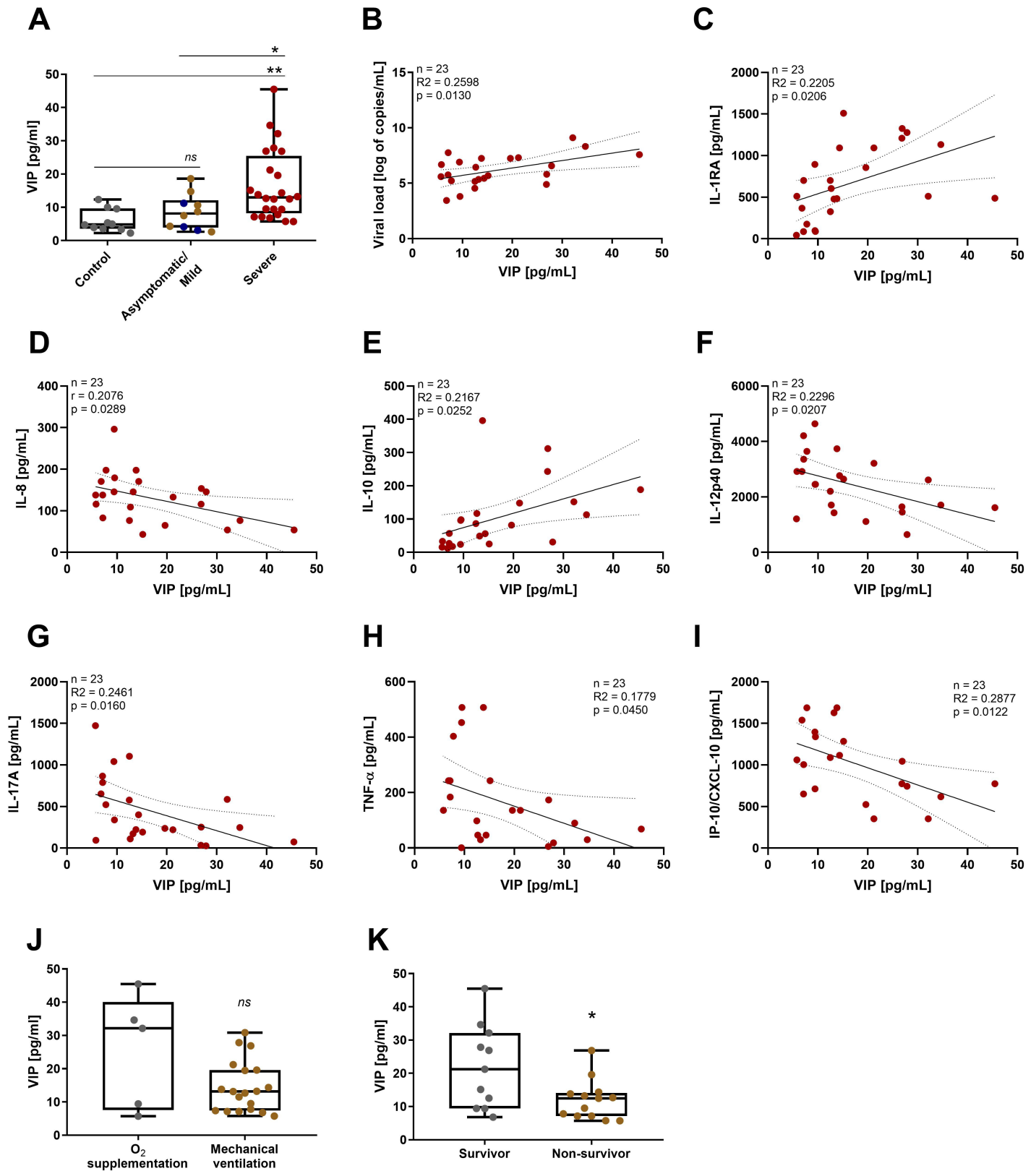
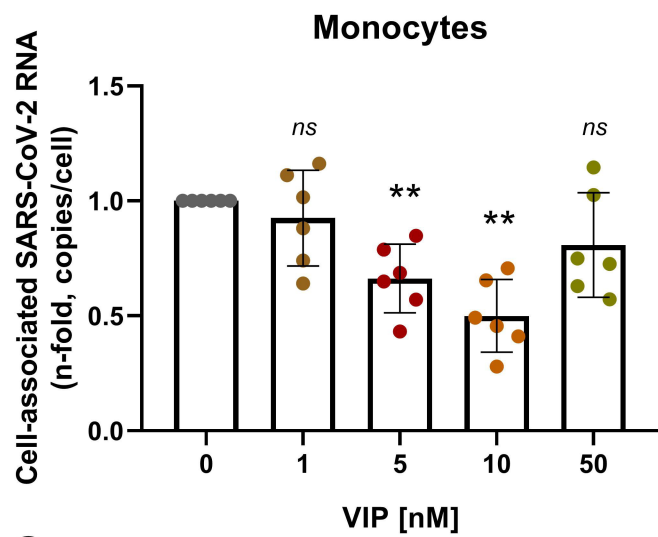
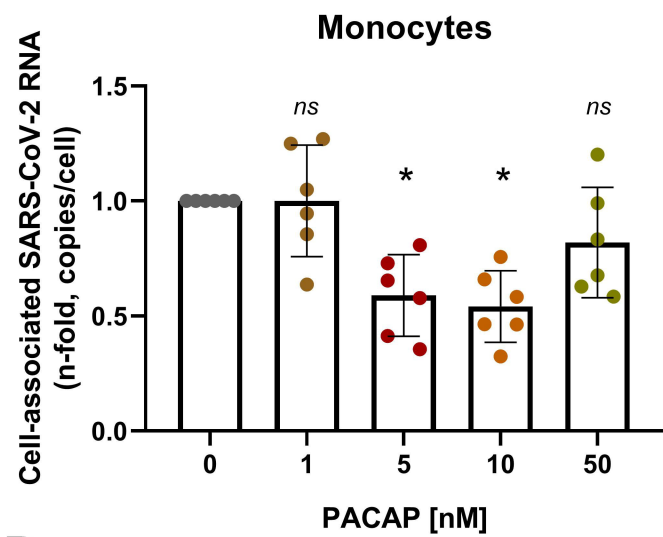


Figure 2

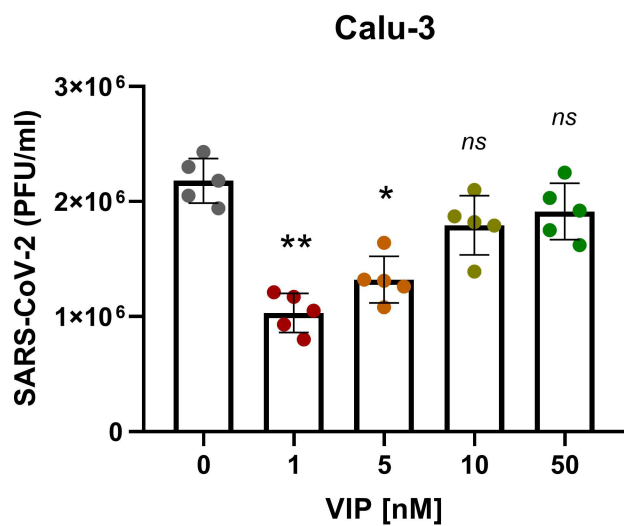
A



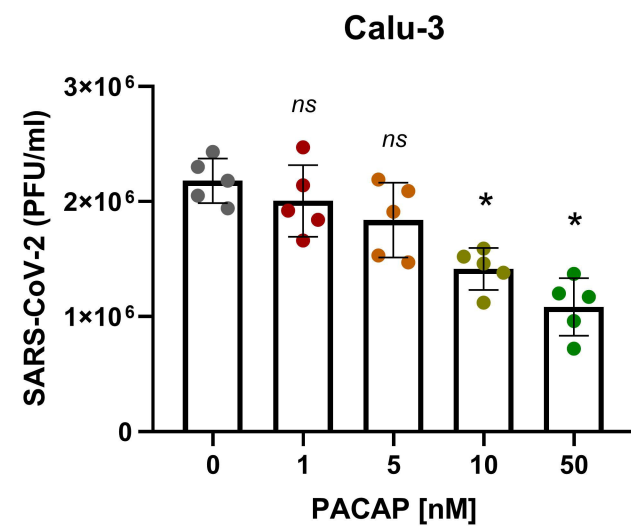
B



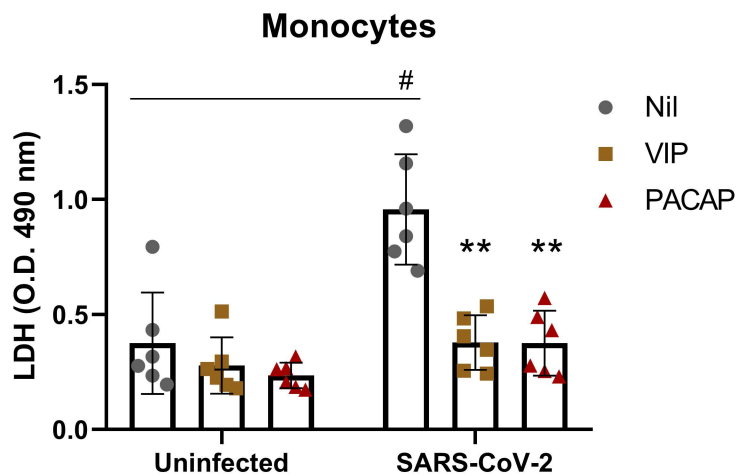
C



D



E



F

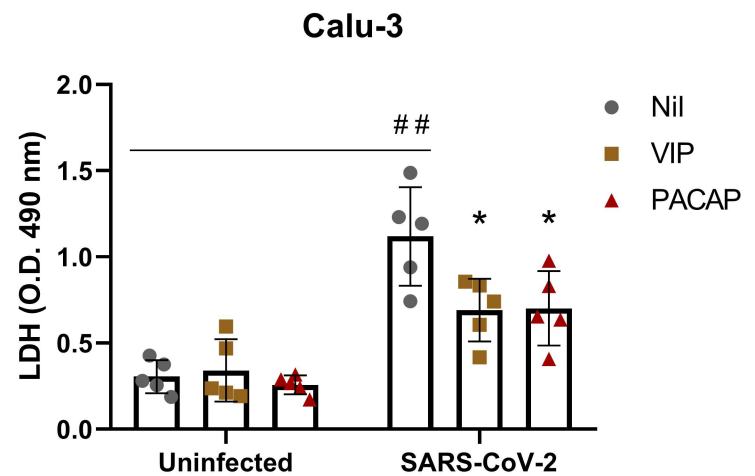
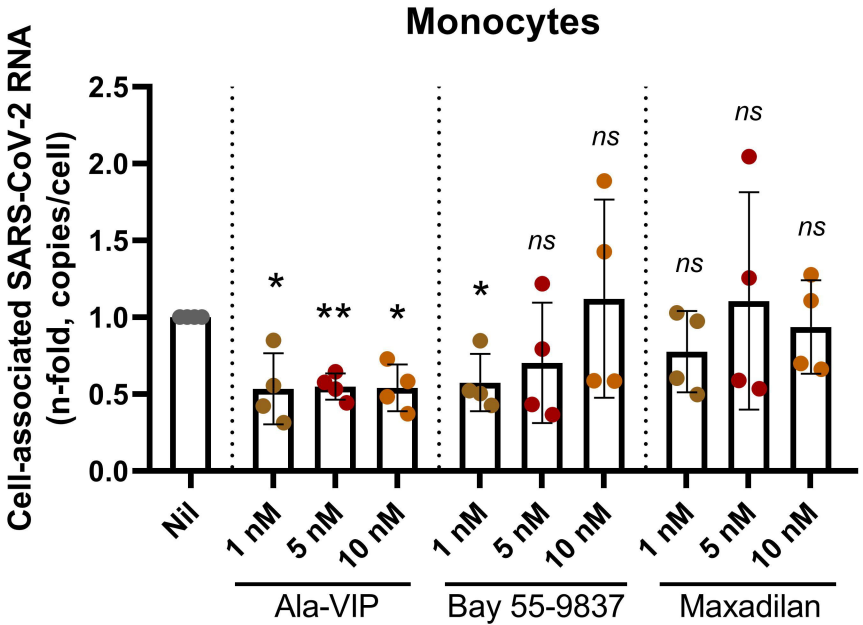


Figure 3

A



B

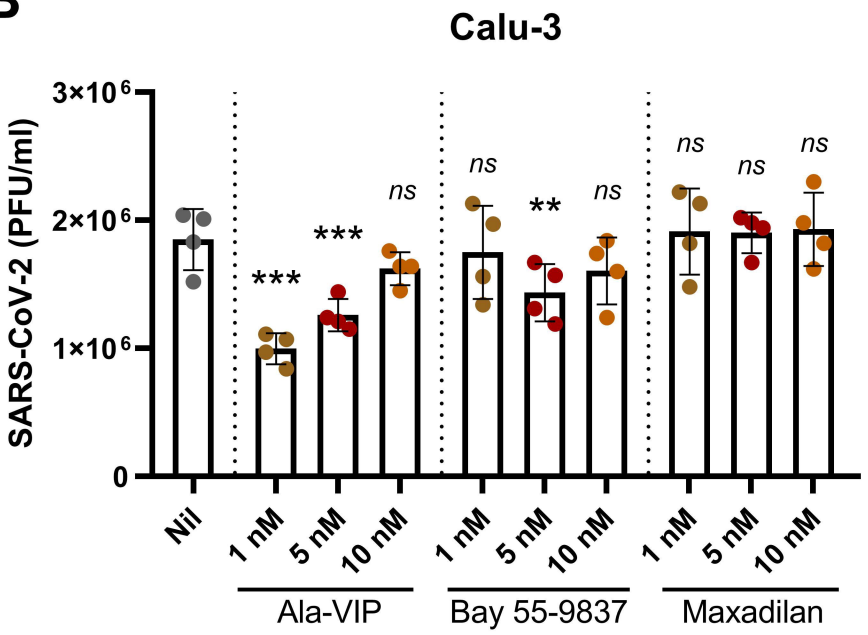
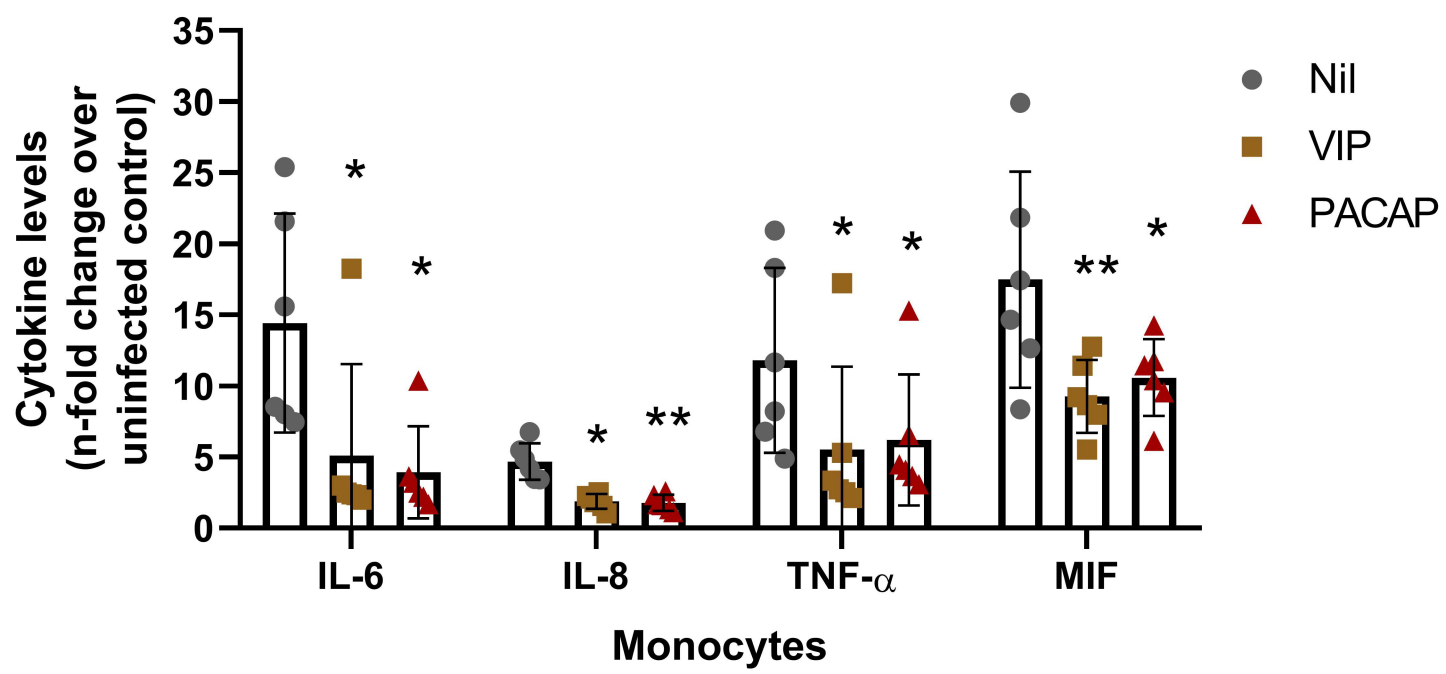


Figure 4

A



B

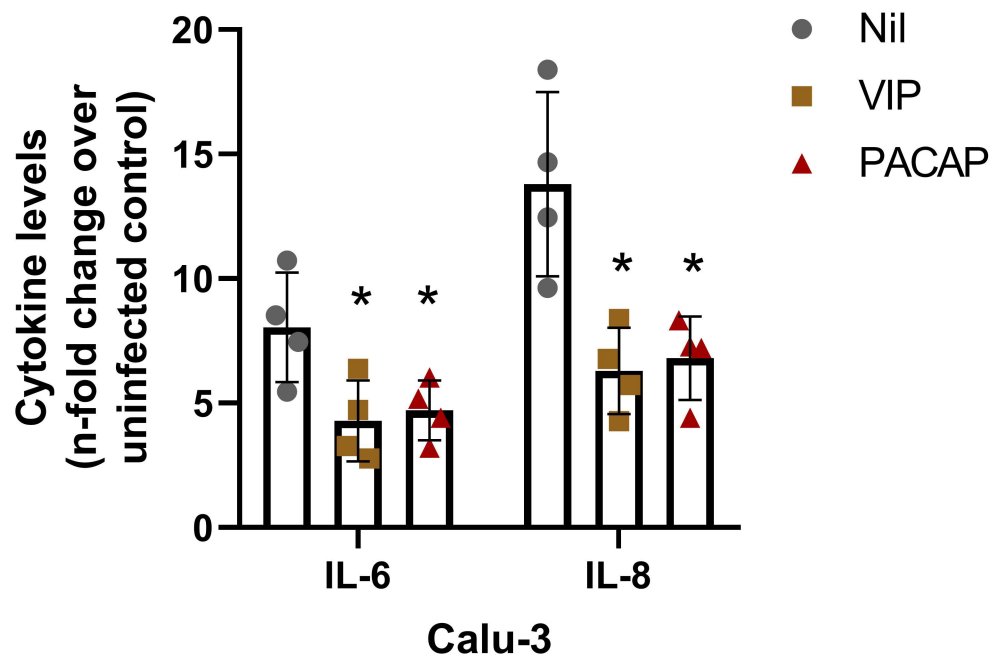


Figure 5

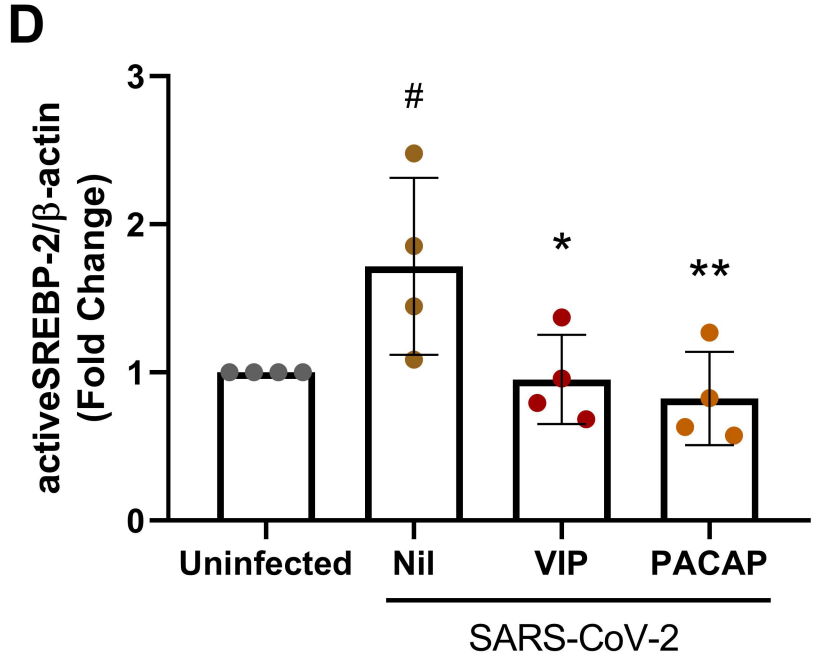
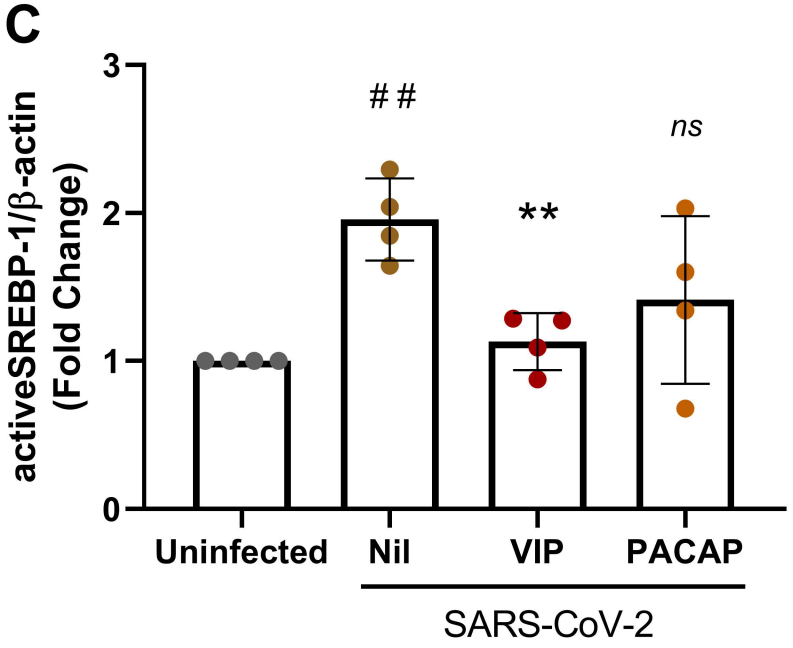
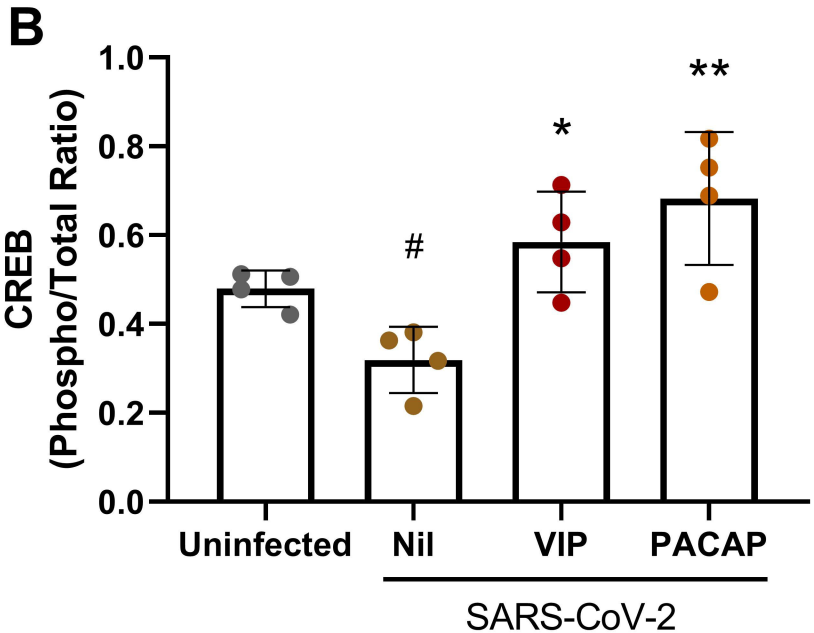
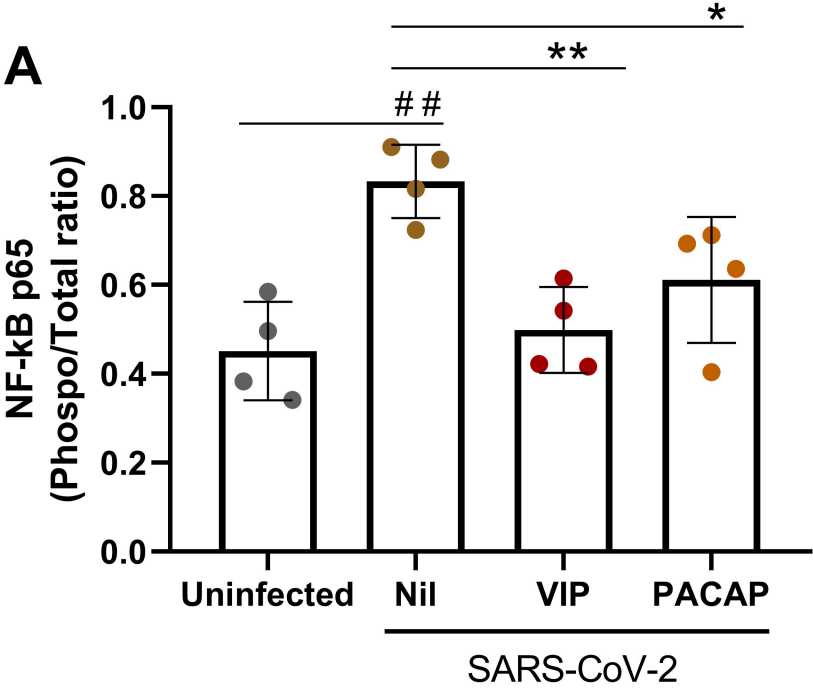


Figure 6

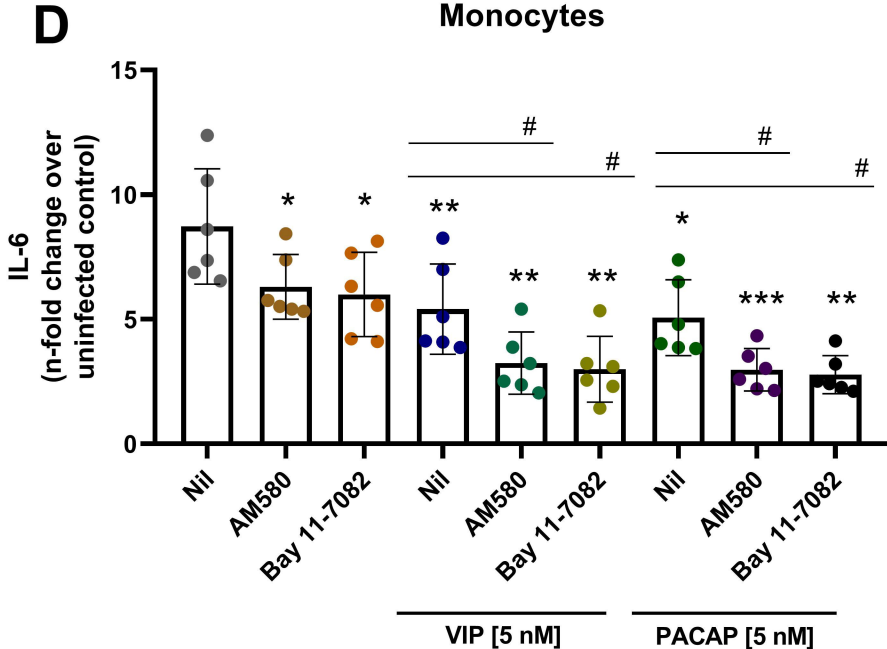
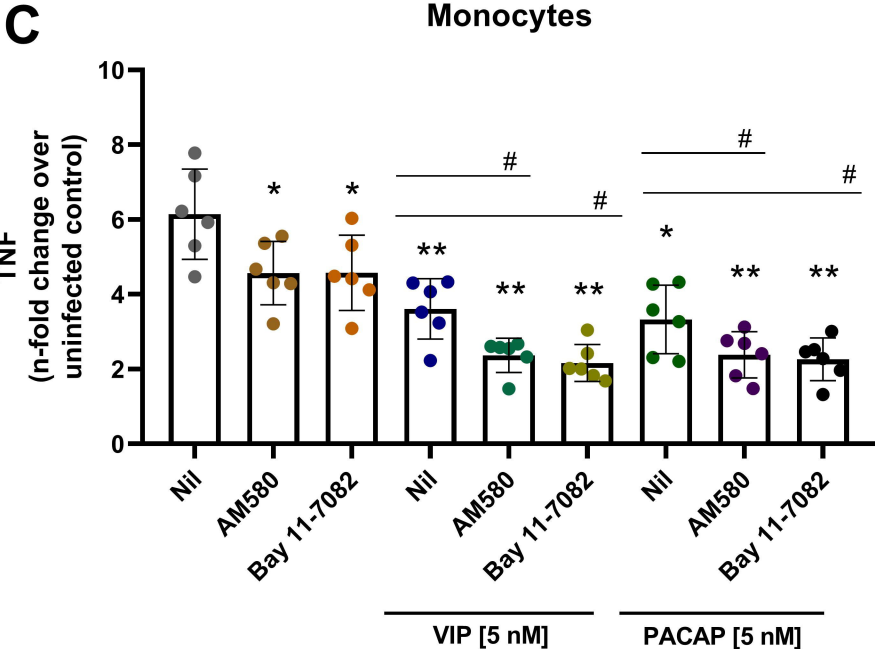
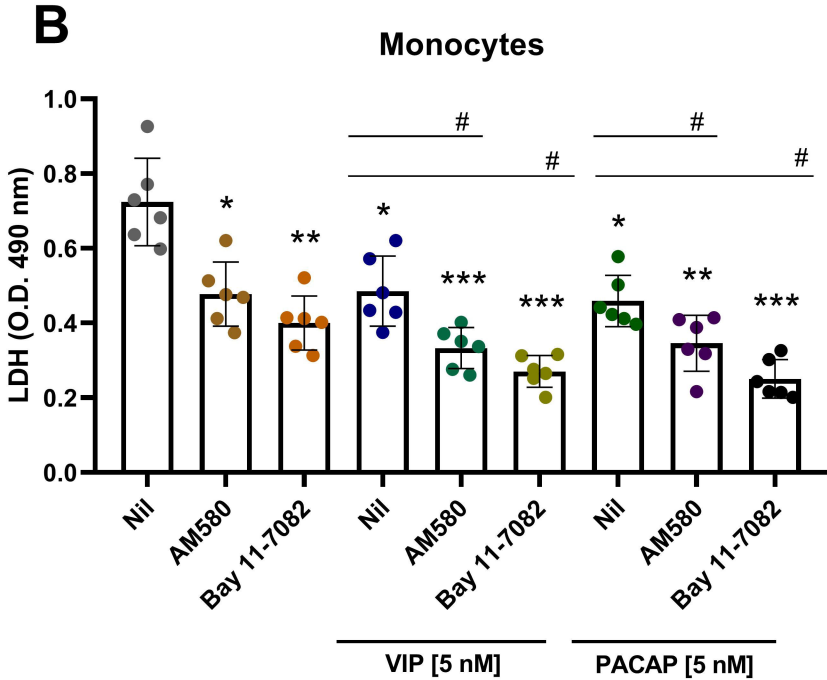
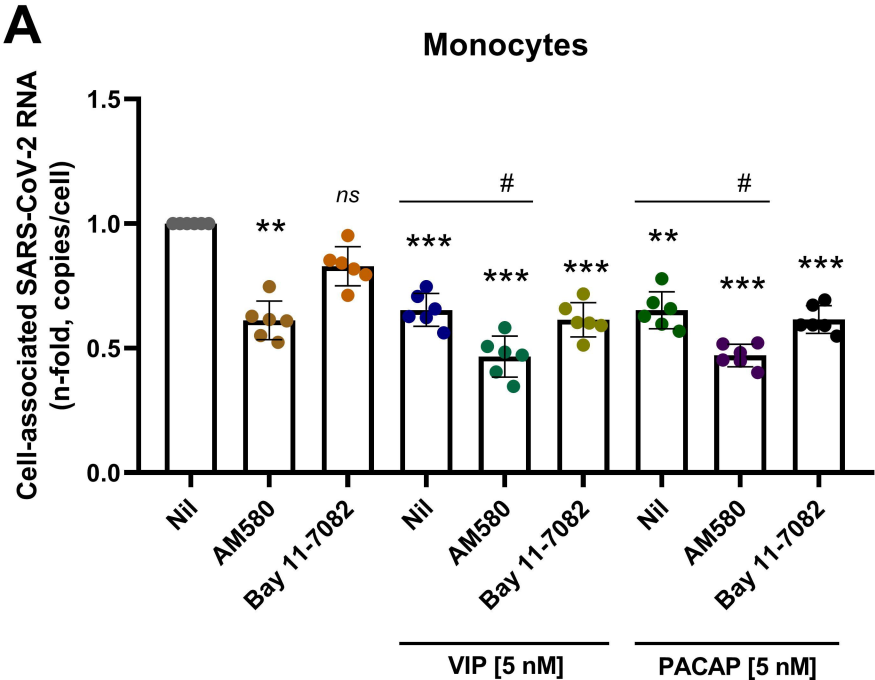


Figure 7

